ISSN 2348-0637
VOLUME 4, 2017

RÜSIE

A JOURNAL OF CONTEMPORARY SCIENTIFIC ACADEMIC AND SOCIAL ISSUES

KOHIMA SCIENCE COLLEGE, JOTSOMA
(An Autonomous Government P. G. College)
NAAC Accredited "A" Grade (1st Cycle, 2011)
NAAC Re-Accredited "A" Grade (2nd Cycle, 2017)

CONTRIBUTORS

Dr. Ralimongla
Associate Professor
Department of Geology
Kohima Science College (Autonomous)
Jotsoma- 797002, Nagaland, India
e-mail: dr.ralimongla@gmail.com

Dr. Lily Sema
Associate Professor
Department of Geology
Kohima Science College (Autonomous)
Jotsoma- 797002, Nagaland, India
e-mail: dr.lilyazha@gmail. Com

T. K. Medowe-u
Assistant Professor
Department of Geography
Kohima Science College (Autonomous)
Jotsoma- 797002, Nagaland, India.
e-mail: medoswuro@gmail.com

Zakali Ayemi
Assistant Professor
Department of Geography
Kohima Science College (Autonomous)
Jotsoma- 797002, Nagaland, India.
e-mail: zakali.ayemi@gmail.com

Dr. S. N. Pandey
Assistant Professor
Department of Mathematics
Kohima Science College (Autonomous)
Jotsoma-797002, Nagaland, India
e-mail: sn_pandey@yahoo.in

Dr. K. Doulo
Assistant Professor
Department of Mathematics
Kohima Science College (Autonomous)
Jotsoma-797002, Nagaland, India
e-mail: kdoulo@rediffmail.com

Dr. Daniel Kibami
Assistant Professor
Department of Chemistry
Kohima Science College (Autonomous)
Jotsoma-797002, Nagaland, India
e-mail: danielkibs80@yahoo.co.in

J. R. Yimchunger
Assistant Professor
Department of Mathematics
Kohima Science College (Autonomous)
Jotsoma-797002, Nagaland, India
e-mail: janeroselineyim@gmail.com

Dr. M. K. Patel
Assistant Professor
Department of Mathematics
National Institute of Technology, Nagaland,
Dimapur-797103, India
e-mail: mkpitb@gmail.com

Neivotsonuo B. Kuotsu
Assistant Professor
Department of Chemistry
Kohima Science College (Autonomous)
Jotsoma-797002, Nagaland, India.
e-mail: solo_berna@yahoo.com

Dr. Vineetha Pillai
Assistant Professor
Department of Chemistry
Kohima Science College (Autonomous)
Jotsoma-797002, Nagaland, India
e-mail: Vineethapillai63@gmail.com

G. K. Gopesh
Bharatiyar University
Coimbatore-641046, India
e-mail: gopeshgk@gmail.com

CONTRIBUTORS

Dr. Meniele K. Nuh
Assistant Professor
Department of Geology
Kohima Science College (Autonomous)
Jotsoma-797002, Nagaland, India
e-mail: menielenuh@gmail.com

Meripeni Ezung
Assistant Professor
Department of Physics
Kohima Science College (Autonomous)
Jotsoma-797002, Nagaland, India.
e-mail: m_ezung@yahoo.com

Imlisunup Ao
Assistant Professor
Department of Physics
Kohima Science College (Autonomous)
Jotsoma-797002, Nagaland, India.
e-mail: imlisunupao@gmail.com

ISSN 2348-0637

CONTENTS Page

GRANULOMETRIC ANALYSIS OF THE TERTIARY ROCKS OF CHANGKI VALLEY, MOKOKCHUNG DISTRICT, NAGALAND

*Ralimongla and **Lily Sema
* & ** Department of Geology, Kohima Science College (Autonomous), Jotsoma- 797002, Nagaland, India
e-mail: *dr.ralimongla@gmail.com & **dr.lilyazha@gmail.com

Abstract: The Changki valley with its spectacularly developed Tertiary sequences occupies the innermost part of belt of Schuppen along the western margin of Nagaland State. The Tertiary sediments of Changki valley, in general, exhibit a range of mineralogical composition from quartzose arenite (Tikak Parbat Formation), lithic arenite (Changki Formation) to feldsphatic-lithic arenite (Tipamsandstone Formation). The grain- size also shows a similar trend from very fine to very coarse and conglomeratic. It exhibits various primary sedimentary structures, such as cross-beddings, ripple marks etc. The granulometric studies indicate an overall influence of shallow marine, beach and river environments for Barail Group, Changki Formation and Tipam Sandstone Formation respectively.

Key words: Granulometric analysis, Tertiary rocks, Changki valley.

Introduction

The present study is an attempt to elucidate the sedimentological attributes and petrologic evolution of the Tertiary rocks developed in Changki Valley,Mokokchung District ,Nagaland (fig.1). The area investigated covers nearly 125 square kilometres bounded between North parallels of 94º 20' and 94º 30' East meridians of 26º 24' and 26º 30' of the Topographic Sheet No.83 G/7 of Survey of India. It includes areas lying near Changki, Longnak,Chungliyimsen, Atuphu, Mangkolemba and Mongchen Villages of Changkikong Range in the Mokokchung District.

Geomorphic features

The Changki valley flanked between two sub-parallel strike ranges – the Changkikong to the east and Japukong to the west, presents an immature geomorphic character. The outer Japukong range attains an average elevation of 750 meters, where as the inner Changkikong range has an average elevation of 1000 meters. The entire area is dissected by three prominent northwest flowing streams namely, Tsusemsa, Longnak and Tsujenyong nalas. The Longnak nala forms the main drainage system and divides the area approximately into two halves. It assumes the name of Tsuing River in the lower reaches which in turn joins the Desai River, an important tributary of Brahmaputra River.

Grain size analysis

Although grain-size of sediments has been understood as an important physical attribute since the beginning of the twentieth century (Wentworth, 1922; Krumbein and Pettijohn, 1938), interest in size characteristics and size frequency distributions has rather assumed greater significance in recent years as evidenced by a large number of published literatures on the subject. Important contributions in this field of study have been made by Folk (1966); Friedman (1967); Visher (1969); Greenwood and Davidson (1976); Tucker and Vacher (1980); Bridge (1981) ; McLaren (1982) and others.

In spite of extensive studies on this subject, much controversy still exists among the workers regarding the effectiveness of many techniques available for discriminating and classifying sedimentary environments. In the preceding sections, grain – size and texture have been described to find possible environment of deposition of the Tertiary sediments under study and to test some of the available techniques for environmental interpretations.

Methodology

Since rocks are hard and compact, thin section technique of grain-size analysis was employed in the present investigation following the method first suggested by Krumbein, (1935). This had been the only available method for the indurated rocks, however, it has been recently improved, employed and justified upon by several workers like Friedman (1962); Stauffer (1966); Conner and Frem (1966); Smith (1966) and Textoris (1971).

Grain-size measurement of 37 (thirty seven) fresh representative samples of different lithofacies types were carried out with eye piece micrometer in regular traverses using mechanical stage fitted with petrological microscope at Wadia Institute of Himalayan Geology, Dehradun. Approximately more than 200 grains were measured in each thin section. The measured grain-size (detrital outline is marked by thin iron-oxide) values were grouped into half-phi intervals and the frequency and cumulative curves were plotted (using ordinary arithmetic graph paper and arithmetic probability paper respectively), for each lithofacies type. Statistical measures of distributions were calculated using formulas suggested by Folk (1974) and later somewhat modified by Friedman and Sanders (1978). Phi values of different percentiles were read from the cumulative curves.

In the present investigation Graphic measures have been preferred to moment measures, because the former is simpler to calculate and generally independent of inaccuracies introduced by truncating and grouping of data (Jones, 1970; Jaquet and Vernet, 1976; Swan, Clague and Luternauer, 1978).

Grain-size distribution, statistical parameters

The data on grain-size distributions and descriptive statistical measures are presented in table 1 and 2 respectively. Representative cumulative curves for different lithofacies types of Barail Group, Changki Formation and Tipam sandstone Formation are plotted in fig.2, 3 &4 respectively. A comparison with the pattern of cumulative curves for various types of environments as suggested by Visher(1969) indicates that the curves for the Tertiary sediments of the area investigated correspond approximately to shallow marine and fluvial sand deposits. A brief account of regional variation of different statistical parameters is given below.

Mean grain-size (M_Z)

It indicates the average grain-size of the depositional basin. The average phi values for the mean size show a decreasing as well as increasing trend towards the south western and north eastern parts of the area respectively in the case of all the litho-types.

Mode (M_O)

It is an important statistical parameter which indicates more on mixing of sediments from several parent deposits. An overall variation of M_O (table 2) suggests that Tertiary sediments in the area are polymodal to bimodal towards north east where as it is a bit unimodal near the south eastern margin of the area.

Standard deviation (σ_1)

It describes the average spread of the distribution curve and reflects the sorting or current and wave condition of the depositional environment. The values of σ_1, in case of all the three Formation studied indicate an improvement in the sorting from south west towards north eastern portion of the area.

Skewness (SK_1)

It measures the deviation of the mean from the median of the grain-size distribution curves. It also gives information about symmetry of the frequency curve. In the north eastern part, distribution are mainly fine-skewed, where as, near symmetrical to coarse skewed dominates toward the south eastern part of the area.

Kurtosis (K_G)

It measures the degree of peakedness of the frequency curve with respect to normal probability curve (K_G =1.00, mesokurtic). On an average, meso- to leptokurtic nature predominates towards south west where as, curves are comparatively platykurtic in the north eastern portion of the area.

Cumulative curve analysis

The Tertiary succession in the study area has been divided into three Formations, namely Tikak Parbat Formation, Changki Formation (newly identified) and Tipam sandstone Formation. These are mostly dominated by interbedded medium to fine sandstones- shale- coal, conglomerate, very coarse to medium sandstones – mud and very coarse to fine calcareous and non-calcareous sandstones-shale sequences respectively. This entire assemblage may be divided into nine lithofacies types including three each from the respective Formations. Following Miall (1990), these lithofacies were assigned specific codes, namely SlfSc ,SpSt & C in respect of Tikak Parbat Formation , GpGt, Sp & fl in respect of Changki Formation and Sprfl, Spr &PSr in respect of Tipam Sandstone Formation.

The representative and average cumulative curves for different lithofacies of Barail Group, Changki Formation and Tipam Sandstone Formation are shown in Figs. 2,3 &4. Based on shape, cumulative curves may be grouped into two types. Type (I) curves have steep and straight segments towards both the ends , but slightly concave middle. These are mostly confined to Tikak Parbat and Tipam Sandstone Formations. Type (II) curves, which are comparatively steeper and straight with minor local truncations, characterise the Changki Formation. In general both the types display a concave - up slope break (C.T-coarse truncation) near 0.25 mm. (+ 2 phi, fine to medium sand) and indicate the transition from transport by traction or surface creep(rolling , sliding etc.) to transport by intermittent suspension (Middleton, 1976). This 2 phi-break corresponds approximately to the mid-point of the transition between Rubey's impact Law and Stoke's Law of particle settling (Sagoe and Visher,1977); Fig.4; p298).A second major slope break , which separates transportation by suspension from intermittent suspension (saltation) , occurs around +3.5 phi (around +4.00 phi in the present case). This break (F.T-fine truncation) lies approximately at silt – clay boundary i.e., lower limit of the transition between Rubey's Impact Law and Stoke's Law. The slight variation in the two principal slope breaks C.T and F.T may be correlated in terms of current velocities, flow separation, flow regimes , velocity gradients , grain shape and densities and fluid density (Sagoe and Visher,1977). The saltation population 'A' is actually transported by intermittent suspension or turbulence caused by velocity fluctuation in water (Lambiase, 1982). The observed shift

towards coarse grain sizes together with steepness of curve segment in case of GpGt, Sp and fl (Changki Formation) reflect a higher energy condition of the depositional environment compared to Tikak Parbat and Tipam sandstone Formation. The probable environments as deduced from the shape of cumulative curves after Visher (1969) are indicated in table 3.

Conclusion

It is generally believed that the regional and stratigraphic variations in grain-size parameters depend on the regional palaeoslope and topographic relief of the depositional site (Friedman, 1967; Amaral and Pryor, 1977). The overall general picture which emerges from the study of such variation is a slight depression towards eastern part and a general palaeoslope towards existence of post Barail sedimentation appears to follow a NE-SW trending palaeo- shoreline with a general paleoslope towards south and east. The post Barail sedimentation led to the deposition of Changki Formation on an undulating erosional surface having a general slope dominantly towards south. The coarsening offshore during this period may be attributed to a lag effect caused due to the landward segregation of relatively finer sands by storm generated waves or strong tidal currents. The Tipam sandstones also experienced the similar conditions except for intermittent subsidence of basin floor towards north eastern part of the basin. On an average, the sorting values for Barail Group, Changki Formation and Tipam sandstone vary between 0.50- 0.86ϕ, 0.32-1.12 ϕ and 0.54-1.0 ϕ respectively, thereby indicating an overall influence of shallow marine, beach and river environments (Folk, 1965).

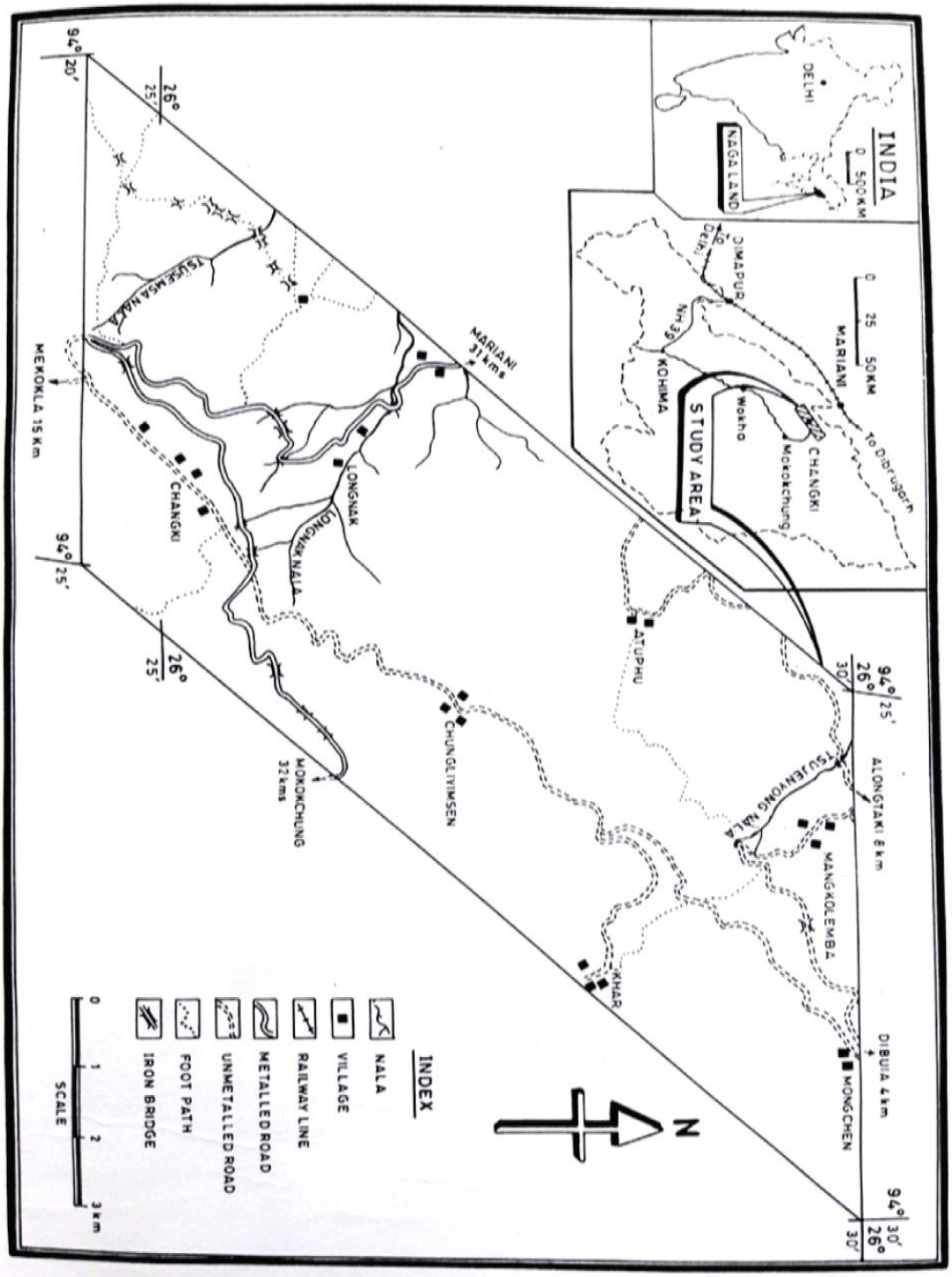

Fig.1: Location map of the area.

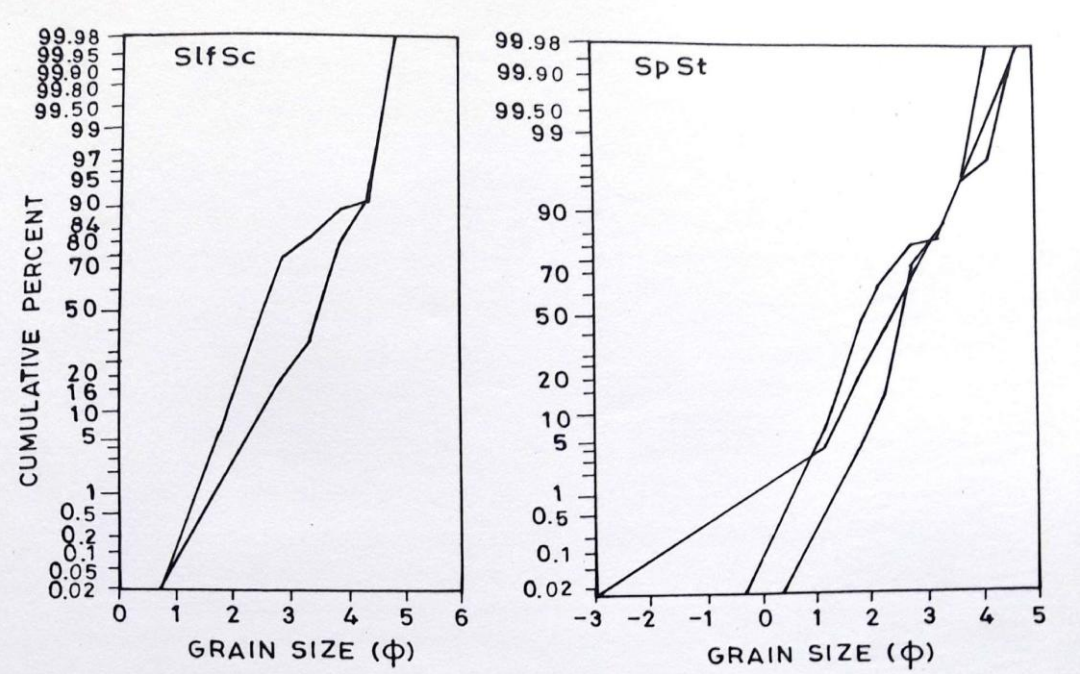

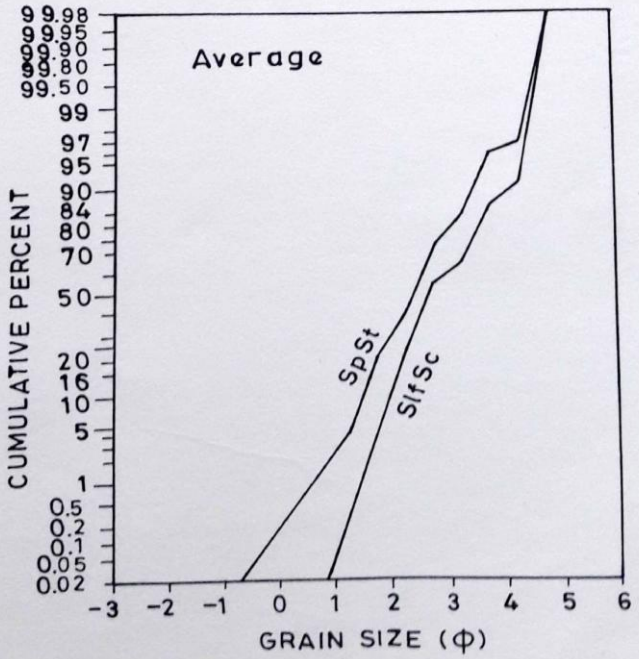

Fig. 2 : Cumulative curves of different facies of the Barail Group.

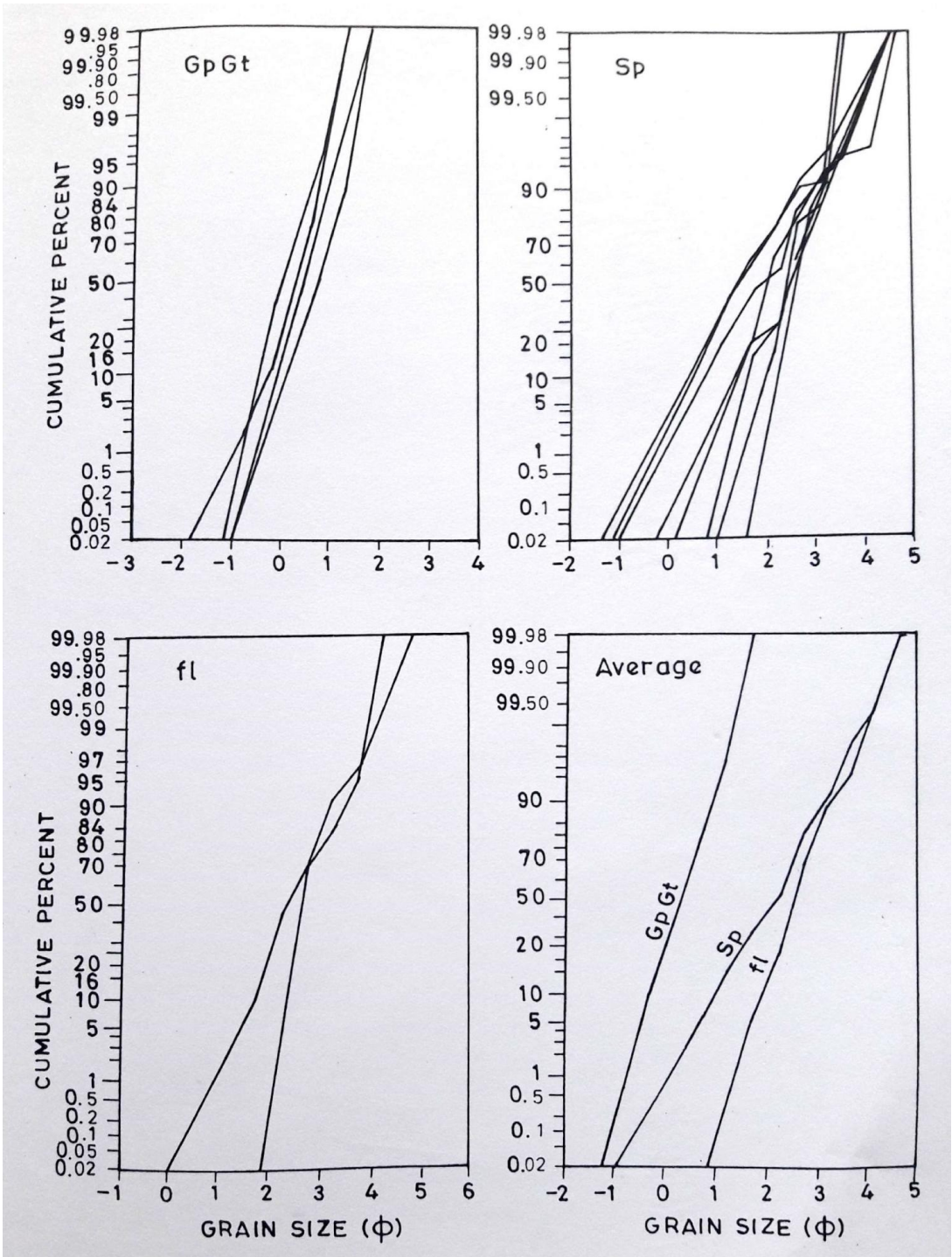

Fig.3 : Cumulative curves of different facies of the Changki Formation.

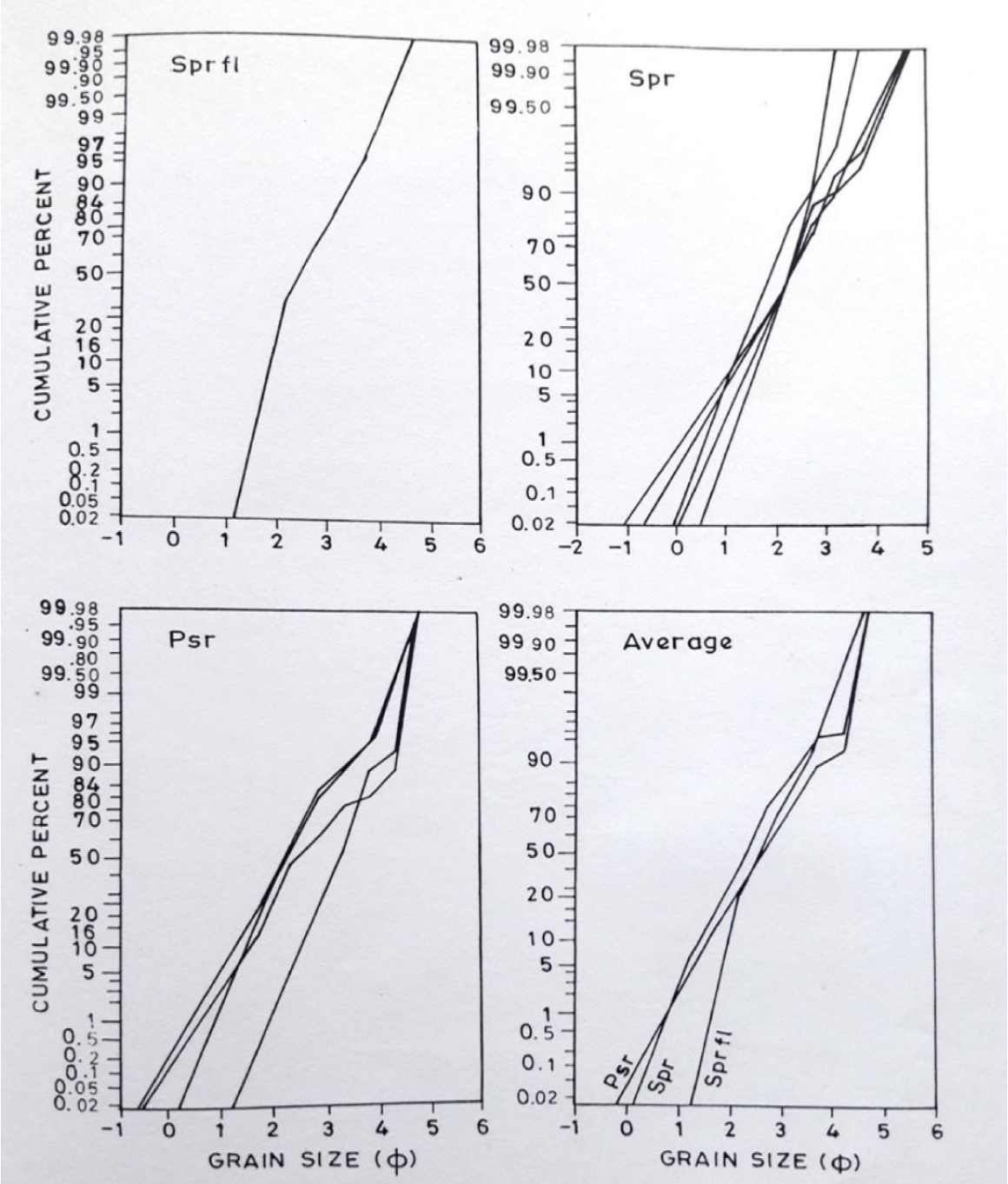

Fig. 4 : Cumulative curves of different facies of the Tipam Sandstone Formation.

Table 1 : GRAIN SIZE FREQUENCY (IN PERCENT) DISTRIBUTION OF DIFFERENT LITHOFACIES OF TERTIARY ROCKS IN CHANGKI VALLEY

CLASS INTERVAL IN PHI-UNITS (mm)	SAMPLE NO. SlfSc				SAMPLE NO. SpSt				
	R94/388	R94/389	R94/391	Average	R92/39	R94/392	R94/393	R94/394	Average
0.50-1.00 (0.707-0.500)	0.00	0.00	0.00	0.00	1.79	0.00	4.00	2.82	2.15
1.00-1.50 (0.500-0.354)	0.00	0.00	0.00	0.00	7.14	0.00	2.00	2.00	2.78
1.50-2.00 (0.354-0.250)	0.00	6.00	7.54	4.51	32.14	4.69	18.00	16.56	17.84
2.00-2.50 (0.250-0.177)	5.66	26.00	26.00	19.22	25.00	10.94	20.00	21.00	19.23
2.50-3.00 (0.177- 0.125)	13.21	42.00	41.25	32.15	14.28	54.69	26.00	27.00	30.49
3.00-3.50 (0.125-0.088)	16.98	8.00	8.00	10.99	3.57	17.19	12.00	13.00	11.44
3.50-4.00 (0.088-0.0625)	45.28	8.00	8.00	20.42	12.50	9.37	14.00	13.60	12.36
4.00-4.50 (0.0625-0.044)	9.43	2.00	2.00	4.47	0.00	0.00	2.00	1.87	0.96
4.50-5.00 (0.044-0.031)	9.43	8.00	8.00	8.47	3.57	3.12	2.00	2.15	2.71
5.00-5.50 (0.031-0.022)	0.00	0.00	0.00	0.00	0.00	0.00	0.00	0.00	0.00

CLASS INTERVAL PHI-UNITS (mm)	SAMPLE NO.						
	GpGt*	*	*	*	**	*	***
	R94/295	R94/297	R94/346	R94/350	R94/365	R94/368	Average
-1.00 - 0.50 (2.00 - 1.414)	1.786	1.695	0.00	1.724		0.00	1.04
-0.5 - 0.00 (1.414 - 1.00)	7.143	5.085	4.762	25.862		0.00	8.57
0.00 - 0.50 (1.00-0.707)	35.714	44.068	28.571	46.552		16.22	34.22
0.50 - 1.00 (0.707-0.500)	44.643	30.508	47.619	22.414	12.15	35.14	36.06
1.00 - 1.50 (0.500-0.354)	10.714	15.254	16.667	3.448	24.00	37.84	16.78
1.50 - 2.00 (0.354-0.250)	0.00	3.39	2.38	0.00	22.15	10.81	3.31
2.00-2.50 (0.250-0.177)					16.4		
2.50 - 3.00 (0.177- 0.125)					14.15		
3.00 - 3.50 (0.125-0.088)					2.15		
3.50 - 4.00 (0.088-0.0625)					4.00		
4.00-4.50 (0.0625-0.044)					1.00		
4.50 - 5.00 (0.044-.031)					4.00		
5.00 - 5.50 (0.031-0.022)							

* Size distribution represents only the coarser fractions of GpGt.
** Size distribution represents only the finer fraction of GpGt.
*** Average of coarser fraction only.

CLASS INTERVAL PHI-UNITS (mm)	Sp SAMPLE NO. R94/300	R94/301	R94/303	R94/304	R94/306	R94/307	R94/308	R94/309
0.50-1.00 (0.707-0.500)	0.00	0.00	0.00	16.90	9.76	0.00	19.23	0.00
1.00-1.50 (0.500-0.354)	5.26	6.06	0.00	24.07	14.63	0.00	23.08	5.00
1.50-2.00 (0.354-0.250)	15.79	15.15	0.00	21.18	21.95	2.44	21.15	10.00
2.00-2.50 (0.250-0.177)	7.89	45.45	6.67	15.42	9.76	17.07	15.38	48.00
2.50-3.00 (0.177- 0.125)	36.84	18.18	53.33	13.47	29.27	58.54	13.46	20.00
3.00-3.50 (0.125-0.088)	23.68	9.09	33.33	1.08	7.32	9.76	0.00	10.00
3.50-4.00 (0.088-0.0625)	10.53	6.06	6.67	4.02	2.44	9.76	3.85	7.00
4.00-4.50 (0.0625-0.044)	0.00	0.00	0.00	1.21	0.00	0.00	0.00	0.00
4.50-5.00 (0.044-0.031)	0.00	0.00	0.00	3.86	4.88	2.44	3.85	0.00

CLASS INTERVAL PHI-UNITS (mm)	SPr SAMPLE NO. R94/276	R94/277	R94/278	R94/279	R94/333	R94/334	Average
0.50-1.00 (0.707-0.500)	0.00	0.00	0.00	0.00	0.00	0.00	0.00
1.00-1.50 (0.500-0.354)	14.28	0.00	8.33	0.00	13.64	0.00	6.04
1.50-2.00 (0.354-0.250)	31.43	16.67	14.58	8.57	15.91	18.37	17.58
2.00-2.50 (0.250-0.177)	31.43	33.33	27.08	25.71	22.73	28.57	28.14
2.50-3.00 (0.177- 0.125)	14.29	25.00	41.67	20.00	34.09	30.61	27.61
3.00-3.50 (0.125-0.088)	8.57	19.44	6.25	22.86	4.54	10.2	11.97
3.50-4.00 (0.088-0.0625)	0.00	2.78	2.08	22.86	4.54	10.2	7.07
4.00-4.50 (0.0625-0.044)	0.00	0.00	0.00	0.00	0.00	0.00	0.00
4.50-5.00 (0.044-0.031)	0.00	2.78	0.00	0.00	4.54	2.04	1.56
5.00-5.50 (0.031-0.022)	0.00	0.00	0.00	0.00	0.00	0.00	0.00

CLASS INTERVAL PHI-UNITS (mm)	PSr SAMPLE NO. R94/332	R94/335	R94/336	R94/374	Average
0.50-1.00 (0.707-0.500)	0.00	0.00	0.00	0.00	0.00
1.00-1.50 (0.500-0.354)	0.00	5.00	9.34	5.26	4.90
1.50-2.00 (0.354-0.250)	0.00	17.15	16.7	10.53	11.18
2.00-2.50 (0.250-0.177)	0.00	30.00	26.36	31.58	21.98
2.50-3.00 (0.177- 0.125)	22.22	27.5	30.79	13.16	23.41
3.00-3.50 (0.125-0.088)	31.11	10.00	7.27	15.79	16.04
3.50-4.00 (0.088-0.0625)	35.56	5.00	4.77	5.26	12.64
4.00-4.50 (0.0625-0.044)	4.44	0.00	0.00	7.89	3.08
4.50-5.00 (0.044-0.031)	6.67	5.00	4.77	10.53	6.74
5.00-5.50 (0.031-0.022)	0.00	0.00	0.00	0.00	0.00

Table 2 : STATISTICAL PARAMETER OF SIZE FREQUENCY DISTRIBUTION OF DIFFERENT LITHOFACIES OF TERTIARY ROCKS IN CHANGKI VALLEY.

SAMPLE NO.	MEDIAN (P50)	MEAN SIZE (Mz)	STANDARD DEVIATION (δI)	SIMPLE SORTING MEASURE (Sos)	SKEWNESS (Sk_I)	SIMPLE SKEWNESS MEASURE (α s)	KURTOSIS (KG)
SlfSc							
R94/388	3.40	3.31	0.63	1.05	-0.12	-0.30	1.22
R94/389	2.50	2.63	0.74	1.30	0.33	1.00	1.64
R94/391	2.50	2.60	0.73	1.35	0.28	0.90	1.70
SpSt							
R92/39	1.90	2.20	0.86	1.30	0.42	1.00	1.12
R94/392	2.55	2.63	0.50	0.90	0.21	-0.60	1.64
R94/393	2.30	2.40	0.83	1.35	0.10	0.10	0.92
R94/394	2.40	2.45	0.77	1.20	0.04	0.20	0.90
GpGt							
R94/295	0.30	0.30	0.38	0.60	0.03	0.20	0.98
R94/297	0.25	0.31	0.46	0.80	-0.08	0.30	0.09
R94/350	0.00	0.02	0.38	0.66	0.20	0.11	0.26
R94/365	1.60	0.68	0.94	1.67	0.23	1.05	1.14
R94/368	0.75	0.75	0.42	0.67	-0.05	-0.15	0.92

Sp							
R94/300	2.50	2.40	0.68	1.02	0.19	-2.95	0.99
R94/301	2.10	2.13	0.59	1.05	0.12	0.30	1.23
R94/303	2.70	2.71	0.32	0.55	0.09	0.10	1.12
R94/304	1.50	1.53	0.90	1.60	0.16	0.80	2.78
R94/306	2.00	1.90	0.89	1.55	-0.07	0.10	1.06
R94/307	2.50	2.60	0.48	0.85	0.31	0.50	1.73
R94/308	1.40	1.46	0.88	1.45	0.10	0.30	1.99
R94/309	2.10	2.21	0.56	1.00	0.21	0.40	1.17
R94/314	2.60	2.53	0.66	1.05	0.09	-0.10	1.23
R94/ 378	2.70	2.63	1.12	1.90	-0.13	-0.60	1.04
R94/381	2.35	2.51	0.69	1.11	0.27	0.40	0.94
R94/383	2.50	2.60	0.64	1.05	0.24	0.50	0.94
Fl							
R94/367	2.60	2.66	0.34	1.17	0.44	0.70	1.78
R94/379	2.50	2.63	0.58	0.92	0.32	0.55	0.95
Spr							
R94/276	1.80	1.86	0.58	0.95	0.11	0.10	0.97
R94/277	2.20	2.26	0.59	0.97	0.20	0.45	0.94
R94/278	2.25	2.11	0.57	1.00	-0.15	-2.50	1.17
R94/279	2.60	2.61	0.60	0.90	-0.15	-0.20	0.67
R94/333	2.20	2.08	0.77	1.40	-0.10	0.10	1.19
R94/334	2.30	2.33	0.65	1.10	0.06	0.20	1.13
PSr							
R94/332	3.20	3.18	0.54	1.00	0.02	0.20	1.26
R94/335	2.20	2.23	0.69	1.22	0.13	0.55	1.26
R94/336	2.20	2.15	0.74	1.35	0.00	0.30	1.23
R94/374	2.40	2.68	1.00	1.55	0.43	0.70	0.98

TABLE 3: PROBABLE DEPOSITIONAL ENVIRONMENTS FOR DIFFERENT LITHOFACIES (AVERAGE) TERTIARY ROCKS IN CHANGKI VALLEY

(DEDUCED FROM CUMULATIVE CURVE ANALYSIS AFTER VISHER, 1969)

*C.T-Coarse truncation point; F.T - Fine truncation point.

Lithofacies		Saltation	Population (A)		Suspension	Population (B)	Surface creep	Population (C)		Probable depositional
	Percent	Sorting	C.T.(Phi)	F.T (Phi)	Percent	Sorting	Mixing A &B	F.T.(Phi)	Percent	Sorting	C.T.(Phi)	Mixing A & C	Environments
BARAIL GROUP													
SpSt	90.00	Excellent	1.25	4.25	2.48	Excellent	Less	>4.75	4.50	Moderate	-0.75	Much	Beach/Dune
SlfSc	69.00	Good	2.25	4.25	7.98	Excellent	Less	>4.75	23.00	Good	1.25	Less	Plunge Zone
CHANGKI FORMATION													
GpGt	>3.00	Excellent	1.25	1.75	___	___	___	___	>97.00	Excellent	-1.25	Much	Beach
		(two population)											
Sp	74.50	Moderate	2.25	4.25	0.48	Good	Less	>4.75	25.00	Moderate	-1.00	Much	Beach
Fl	90.50	Good	2.25	3.75	4.48	Good	Much	>4.75	5.00	Good	0.75	Much	Beach/Shoal
TIPAM SANDSTONE FORMATION													
PSr	74.00	Moderate	1.75	4.25	6.98	Excellent	Less	>4.75	19.00	Moderate	-0.25	Much	Beach/Tidal inlet
Spr	89.00	Good	1.25	4.25	3.98	Excellent	Less	>4.75	7.00	Excellent	0.25	Much	Beach/Dune
Sprfl	62.00	Good	2.25	3.75	6.98	Good	Much	>4.25	31.00	Excellent	1.25	Less	Plunge Zone

References

Acharyya, S. K. (1982). Structural framework and tectonic evolution of the eastern Himalaya. Him. *Geol*. **10**: 412-439.

Agrawal, O. P. (1984). Geology of the Nagaland ophiolit and its relation to the Indian plate margin. *Abstract Proc. Seminar on "Cenozoic crustal evolution of the Indian plate margins*". 19.

Amaral, E. J. and Pryor, W. A. (1977). Depositional environment of the St. Peter sandstone deduced by textural analysis. *Jour. Sediment. Petrol*. **47**: 32-52.

Bridge, J. J. (1981). Hydraulic interpretation of grain-size distributions using a physical model for bed load transport. *Jour. Sediment. Petrol*. **51**: 1109-1124.

Connor, C. W. and Ferm, J. C. (1966). Precision on linear and aerial measurements in estimating grain size. *Jour. Sediment. Petrol*. **36**: 397-402.

Evans, P. (1932). Tertiary succession in Assam. Trans.M.n. *Geol. Inst. India*. **37**: 155-260.

Folk, R. L. (1966). A review of grain size parameters. *Sedimentology*. **6**: 73-93.

Folk, R. L. (1974). Petrology of sedimentary rocks. 170 p. Hemphill's Austin: Texas.

Friedman, G. M. (1962). On sorting, sorting coefficient and the log normality of the grain-size distribution of sandstones. *Jour. Geol*. **70**: 737-753.

Friedman, G. M. (1967). Dynamic processes and statistical parameters compared for size frequency distribution of beach and river sands. *Jour. Sediment. Petrol*. **37**: 327-354.

Friedman, G. M. and Sanders, J. E. (1978). *Principal of sedimentology*. 792p. Wiley: New York.

Greenwood, B. and Davidson- Arnott, R. G. D. (1972). Textural variation in sub-environments of the Shallow water wave zone, Kouchibouguac Bay, New Brunswick. *Can. Jour. Earth Sci.* **9**: 679-688.

Jaquet, J. M. and Vernet, J. P. (1976). Moment and graphic size parameters in sediments of Lake Geneva, Switzerland, *Jour. Sediment. Petrol*. **46**: 305- 312.

Jones, T. A. (1970). Comparison of the descriptions of sediment grain size distributions. *Jour. Sediment. Petrol*. **4**: 204-1215.

Krumbein, W. C. (1935). Thin section mechanical analysis of indurated sediments. *Jour. Geol.* **43**: 482-496.

Krumbein, W. C. and Pettijohn, F. J. (1938). Manual of sedimentary petrography. 549p. Appleton-Century-Crofts: New York.

Lambiase, J. J. (1982). Turbulence and the generation of grain-size distribution. Abstracts, 11th international congress on sedimentology, Hamilton, 80-81.

McLaren, P. (1982). Grain size statistics; A new look at their meaning. Abstract, 11th International Congress on sedimentology, Hamilton. 80.

Moss, A. J. (1972). Bed-load sediments. Sedimentology. **18**: 159-219.

Sagoe, K. O. and Visher, G. S. (1977). Population breaks in grain size distributions of sand-A theoretical model. *Jour. Sediment. Petrol*. **47**: 285-310.

Smith, R. (1966). Grain size measurement in thin section and in grain mount. *Jour. Sediment. Petrol*. **36**: 841-843.

Stauffer, P. H. (1966). Thin section size analysis: A further note. *Sedimentology*. **7**: 261-263.

Swan, D., Clague, J. J. and Luternauer, J. L. (1978). Grain –Size statistics In: Evaluation of the Folk and Ward graphic measures. *Jour. Sediment. Petrol*. **48**: 863-878.

Tanner, W. F. (1964). Modification of sediment size distributions. *Jour. Sediment. Petrol*. **34**: 156-164.

Textoris, D. A. (1971). Grain size measurement in thin section. In : Carver, R. E., ed., *Procedures in sedimentary petrology*. 95-108. Wiley: New York.

Tucker, R. W. and Vacher, H. L. (1980). Effectiveness of discriminating beach, dune and river sands by moments and cumulative weight percentages. *Jour. Sediment. Petrol*. **50**: 165-172.

Visher, G. S. (1969). Grain size distributions and depositional processes. *Jour. Sediment. Petrol*. **39**: 1074-1106.

Wentworth, C. K. (1922). A scale of grade and class terms for clastic sediments. *Jour. Geol*. **30**: 377-392.

SOCIO-ECONOMIC IMPACTS OF EDUCATIONAL INSTITUTIONS ON PRIVATE HOSTELS IN PHEZU AREA, JOTSOMA

*T. K. Medowe-u & **Zakali Ayemi
* & ** Department of Geography, Kohima Science College (Autonomous), Jotsoma- 797002, Nagaland, India.
e-mail: *medoswuro@gmail.com, **zakali.ayemi@gmail.com

Abstract: This paper investigates the socio-economic impact of private hostels in the Phezu area with the mushrooming of educational institutions. Growth of educational institutions has led to the increase of private hostels which is an important determinant of individual earnings and economic growth of the community. In addition, it exhibits long term positive economic and social influence. This region has high potential to grow and develop as an educational hub which will further bring development to the neighboring areas.

Key words: Socio-Economic**,** Educational Institution, human capital, income, employment.

Introduction

The term "socio-economic" may broadly be defined as the use of economics in the study of society. In general, it analyses how societies progress, stagnate or regress because of their local or regional economy or the global economy. It deals with the way economic activities influence and shape social processes. Educational institutions are considered as an agency helping economic production. Therefore, the purpose of studying socio-economic benefits of educational institutions on private hostels in Phezu area is to get an insight of the economic geography of the prevailing area and in turn the social change produced in the region.

Objective

The purpose of the study is to analyze and identify socio-economic benefits offered to the community through mushrooming of educational institutions in the Phezu area. It includes long term impacts on the prevailing socio-economic conditions obtained by private hostels due to the location of educational institutions.

Data and method

The study is inductive and empirical based on both primary and secondary data. Primary Data includes field visits, observation, and personal interview, collecting of relevant data and information from unpublished materials and sources and through questionnaires in the study area. Secondary Data includes published materials like books, magazines, articles/ literature/ internet/ websites. Quantitative tools and techniques are applied for data analysis.

Study area

Location

The study area "Phezu" locality is an extension of Jotsoma Village under Tholoma Khel, Kohima district, Nagaland. It lies between 25°67'N - 25°65'N latitude and 94°6'E-94°8'E longitude. The area is located at an altitude of about 1200m-2250m above sea level. It is situated 6 km away from the capital of the state, Kohima. It is bounded by Jotsoma village in the north, Forest and Paramedical

Colony of Kohima in the east, Pulie Badze in the south and Ao Christian Fellowship, Agape Hostel and Calvary Baptist Church towards the west.

Map of the Study Area

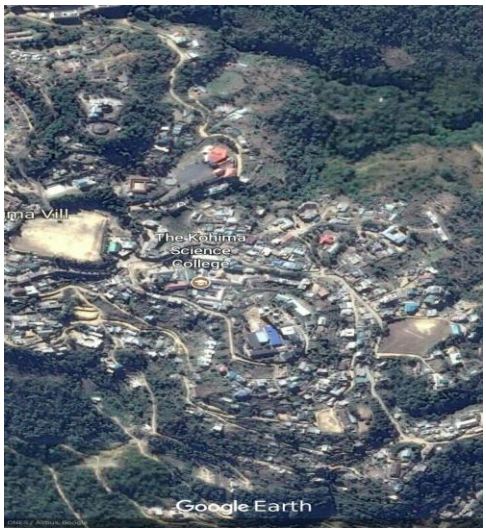

Topography and geology

Topographically, Phezu is located on the sloping terrain of folded mountain Pulie-badze. It is hilly with rugged steep slope. Beds of Mudstone, Sandstone, Clay and Silty Shales of high concentration of Quartz, Micaceous and Siliceous belonging to the Barial formation are found in the area.

Drainage

The area has Chiru River running from the South to North and several other streams that run only during the rainy season. Some of the rivers and perennial streams that pass through and surrounding the area are Dzüna, Tsiesegerü, Lorü, Dzüdza and Dzüchie. River Dzüna is the main source of water supply to the Phezu area, Jotsoma village and Kohima.

Climate

Phezu area has severe winters and warm summers accompanied by rain and wind. The coldest months are from December to February. The temperature ranges from 27°C-32°C during the summer months of June to August, like that of Kohima. During winters, the temperature falls as low as 4°C. It experiences pleasant climatic conditions throughout the year. The annual temperature ranges from below 5°C- 10°C in winter and 14°C-28°C in summer. The rainfall in the study area starts by the end of March and continues till the Mid October. According to the rainfall data collected by the Meteorological Department, Kohima, Nagaland; the highest rainfall is recorded in the months of June, July and August every year ranging from 220mm-440mm per day.

Flora and Fauna

The area falls under temperature evergreen forest. The common floras of the region are Ginseng, silk cotton, wild apple, rhododendron, gooseberry, alder etc. The fauna of the region consists of mithun, tragopan, house sparrow, bamboo rat, cattle crow, green pigeon, etc.

Analysis and findings

Educational Institutes

There are altogether seven educational institutions concentrated in Phezu locality, along with one Day care center/

Kindergarten; one Government Primary School, one Government High School, two Higher Secondary School of private unaided establishment, One Private College and One Government Post Graduate Autonomous College namely: Sazolie college and Kohima Science College (Autonomous). The literacy rate of the area is around 70-75%. Name of the Educational institutions are listed below with their details:

Table1: Educational Institutions and year of establishment

Name of the institute	**Type of institute**	**Govt\Pvt**	**Year of Estd**	**Total enrolment of students in the current year**
Kohima Science College	College	Govt	1961	1358
Govt High School	High school	Govt	1968	140
Govt Primary School	Primary	Govt	1970	66
Charles Dewitt King Hr. Sec School	Higher Secondary	Private unaided	1973	250
Aldervile School	High school	private	1992	290
Sazolie	College	Private	2005	430
Bright Beginnings	Day Care Center	Private	2016	19

Private Hostels

There are thirty-one hostels concentrated in Phezu locality. Of which twenty-nine are private (eighteen hostels are boys hostel and eleven girls hostels) and four Government hostels (one for girls and three for boys). Twenty-two of the hostels have R.C.C buildings while the rest seven have Assam type buildings. The occupants in the hostels are from the nearby educational institutions i.e. Kohima Science College and Sazolie College as the intake capacity of these institutions are more. Also, some of the occupants are civil service aspirants. According to the study, it has been found out that with the increase in the educational institutions, there has been increased enrollment of students. This in turn led to further establishments of hostels to accommodate the growing needs of the demand.

Table 2: Decadal growth of Hostels

Decade	Boys Hostel	Girls Hostel	Total Number of Hostels Established
1980-1990	1	0	1
1991-2000	4	3	7
2001-2010	7	6	13
2011-2017	6	2	8
Total	**18**	**11**	**29**

Trend in the growth of Hostels

The first private hostel i.e. Don Bosco Hostel was established in the year 1989. Though the establishment of hostel in the first decade was only one, from 1990-2000 seven new hostels were established, thirteen hostels were established from 2001-2010, and from 2011-2017 eight hostels came up. From the given statistics, it can be concluded that with the expansion of educational institutions, there is a significant rise of private hostels in the region. The below Graph1 shows the trend line of the

growth of private hostels from 1985 to the current year. Graph 2 shows the year of establishment educational institutions. The graphs clearly indicate co-relation between the growth of the private hostels and increase in the establishment of educational institutions.

Graph1: Trend in the growth of hostels

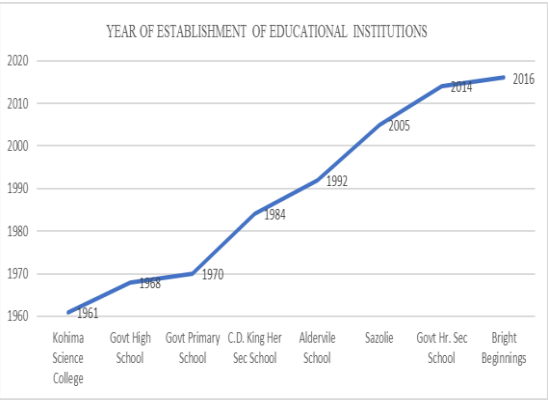

Graph 2: Trend in the year of growth educational institutions

Income generated by hostels

According to the finding, all the hostels are run by the locals from Jotsoma village except Don Bosco Boys Hostel. The aggregate monthly income of the twenty-nine hostels is Rs.18,90,750. While the average monthly income is Rs.65198.28. The range of the income is between Rs.8000-180,800. Lapis Lazuli girls hostel has the highest monthly income of Rs.1,80,800. The monthly fees of this hostel is higher comparatively to other hostels, it has better infrastructure and facilities, and provides both single and double seater rooms. The lowest monthly income is Rs.8000 from Bros hostel. While the maximum of the hostels generates income in the range between Rs.31000-60,000.

Table 3: Income of hostels per month in Rupees

Income in rupees	No of Hostels
0-30000	5
31000-60000	11
61000-90000	7
90000-120000	6

Employees

There are fifty-four employees including wardens, cooks and helpers, of which forty- nine are locals while only five are non-locals. The total numbers of female employees are thirty-one while the male is twenty-three. Through the finding, it can be observed that private hostels are also a source of employment generation especially for the locals.

Table 4: Total Number of Employees

TOTAL	54
Local	49
Non-local	5

*local = people from Jotsoma village

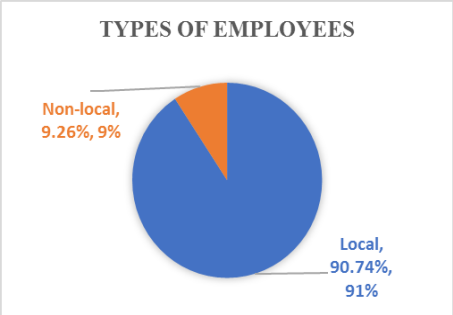

Graph 3: Percentage of Local and Non-Local Employees

Conclusion

Educational Institutions are a vital source of income for the private hostels in Phezu locality. It is due to the location of numerous educational institutions especially the two colleges i.e. Kohima Science College and Sazolie, a vast number of students from all over Nagaland come to study. However, the dearth of accommodation facilities available in their respective colleges, has led to increasing demand and growth of private hostels. It is found that private hostels generate huge income for the locals. Additionally, it is a source of employment for the locals. As per the study, 90% (approx.) of the employees are locals while the rest are non-locals. Thus, the establishment of private hostels plays a significant role in the economy of the Phezhu area. The locality is not only benefitting economically but socially as well. It has contributed to the literacy rate of the area. Development of many small businesses establishments like grocery store, restaurant, hotel, stationary shop, cyber café etc. The locality is also well-connected to the capital due to the establishment of the institutions. Additionally, location of educational institutions is also one of the major contributing factors of migration of skilled people to this area. Assimilation of it, adds to the human capital and socio-economic development of the locality. The positive correlations thus exist between location of educational institution and economy. With the possibility of expansion of educational institutions, there is a huge scope for the region to become educational hub which will further contribute to the socio-economy of the region as well as nearby areas.

Acknowledgement*: The authours would like to thank the Department of Geography and the students of 3rd Semester, Geography for successfully carrying out the survey and helping them with the data.*

References

Morgan, C & Goh Cheng Leong Gillian (1982); Human and Economic Geography. *Population and human diversity.* **1**: 5-40.

Mukherjee and Sampat (2005). Modern Economic Theory. *Economic Growth and Development.* **44**: 927-973.

Roy and Prithwish (2007). Economic Geography. *Human Resources.* **12**: 119-148.

Saxena, H. M. (2004). Marketing Geography. *Marketing and Changing Social Structure.* **16**: 315-330.

Sebu and Soyhunlo (2013). Geography of Nagaland. *Physical Setting.* **2**: 25-44.

Singh, R. Y. (2013). Geography of Settlements. *Culturo-Historical Perspective*. **2**: 73-82.

GENERALIZED QUASI-CONFORMAL CURVATURE TENSOR ON LP-SASAKIAN MANIFOLDS

*S. N. Pandey and **K. Doulo
* & ** Department of Mathematics, Kohima Science College (Autonomous), Jotsoma-797002, Nagaland, India
e-mail: *sn_pandey@yahoo.in

Abstract: The object of the present paper is to study generalized quasi-conformal curvature tensor on LP- Sasakian manifolds.

Keywords: Riemannian manifold, conformal curvature tensor, LP-Sasakian manifold, Einstein manifold, Projective curvature tensor

Introduction

Yano and Sawaki (1972) introduced quasi-conformal curvature tensor in a Riemannian manifold as follows:

$$C(X,Y,Z) = a\,R(X,Y,Z) + b\,[\,S(Y,Z)X - S(X,Z)Y + g(Y,Z)QX - g(X,Z)QY] - \frac{r}{n}\left[\frac{a}{n-1} + 2b\right][\,g(Y,Z)\,X - g(X,Z)\,],$$

where a and b are real constants such that $a, b \neq 0$. R, S, and r are curvature tensor, Ricci tensor, and scalar curvature respectively and X, Y, Z, and W are arbitrary vector fields. Also $'C(X,Y,Z,W) = g(C(X,Y,Z),W)$, $'R(X,Y,Z,W) = g(R(X,Y,Z),W)$, and $S(X,Y) = g(QX,Y)$.

Properties of quasi conformal curvature tensor have been studied by many researchers. Recently Prasad, Doulo and Pandey (2011) introduced and studied generalized quasi-conformal curvature tensor in the context of Riemannian manifold.

Generalized quasi-conformal curvature tensor G for n>3 is defined as

$$G(X,Y,Z) = a\,R(X,Y,Z) + b\,[\,S(Y,Z)X - S(X,Z)Y\,] + c\,[\,g(Y,Z)QX - g(X,Z)QY] - \frac{r}{n}\left[\frac{a}{n-1} + b + c\right][g(Y,Z)\,X\,g(X,Z)\,], \quad (1.1)$$

where symbols have their usual meanings and $a, b, c \neq 0$.

It can be easily verified that

$'G(X,Y,Z,W) + 'G(Y,X,Z,W) = 0$;
$'G(X,Y,Z,W) + 'G(X,Y,W,Z) = 0$

and $'G(X,Y,Z,W) + 'G(Y,Z,X,W) + 'G(Z,X,Y,W) = 0$,

where $'G(X,Y,Z,W) = g(G(X,Y,Z),W)$.

If b=c, then (1.1) takes the form

$$G(X,Y,Z) = a\,R(X,Y,Z) + b[\,S(Y,Z)X - S(X,Z)Y + g(Y,Z)QX - g(X,Z)QY] - \frac{r}{n}\left[\frac{a}{n-1} + 2b\right][\,g(Y,Z)\,X - g(X,Z)\,] = C(X,Y,Z),$$

where C(X,Y,Z) is the quasi-conformal curvature tensor (Yano and Sawaki,1972). Thus the quasi-conformal curvature tensor C is a particular case of the tensor G. For this reason G is called generalized quasi-conformal

curvature tensor (Prasad, Doulo, Pandey, 2011).

An n-dimensional differentiable manifold M^n is a Lorentzian para–Sasakian (LP –Sasakian) manifold, if it admits a (1,1) – tensor ϕ, a vector field ξ, a 1- form η and a Lorentzian metric g which satisfies

$$\phi^2 X = X + \eta(X)\xi \quad \text{and } \eta(\xi) = -1 \tag{1.2}$$

$$g(\phi X, \phi Y) = g(X,Y) + \eta(X)\,\eta(Y) \tag{1.3}$$

$$g(X,\xi) = \eta(X) \tag{1.4}$$

$$(D_X\phi)(Y) = g(X,Y)\xi + \eta(Y)X + 2\eta(X)\,\eta(Y)\,\xi \tag{1.5}$$

$$D_X\xi = \phi X, \tag{1.6}$$

for arbitrary vector fields X and Y, where D denotes the operator of covariant differentiation with respect to the Lorentzian metric g, (Matsumoto,1989) and (Matsumoto & Mihai,1988).

In an LP-Sasakian manifold M^n with structure (ϕ,ξ,η, g), it is easily seen that

(a) $\phi\xi = 0$ (b) $\eta(\phi X) = 0$

(c) rank $\phi = n-1$ (1.7)

Let us put

$$F(X,Y) = g(\phi X,Y) \tag{1.8}$$

Thus we have

$$F(X,Y) = F(Y,X) \tag{1.9}$$

$$F(X,Y) = (D_X\eta)(Y) \tag{1.10}$$

$$(D_X\eta)(Y) - (D_Y\eta)(X) = 0 \tag{1.11}$$

An LP-Sasakian manifold M^n is said to be an Einstein manifold if its Ricci tensor S is of the form

$$S(X,Y) = (n-1)\,g(X,Y) \tag{1.12}$$

Let M^n be an n-dimensional LP-Sasakian manifold with structure (ϕ,ξ,η,g). Then we have

$$g(R(X,Y,Z),\xi) = \eta(R(X,Y,Z)) = g(Y,Z)\,\eta(X) - g(X,Z)\,\eta(Y) \tag{1.13}$$

$$R(X,Y,\xi) = \eta(Y)X - \eta(X)Y \tag{1.14}$$

$$S(X,\xi) = (n-1)\,\eta(X) \tag{1.15}$$

$$S(\phi X,\phi Y) = S(X,Y) + (n-1)\eta(X)\,\eta(Y) \tag{1.16}$$

for any vector fields X,Y,Z and other symbols have their usual meanings (Matsumoto,1989) and (Matsumoto & Mihai, 1988).

Einstein LP-Sasakian manifold satisfying (div G) (X,Y,Z) = 0

Definition(2.1): A manifold (M^n, g) is called generalized quasi conformally conservative if (div G) (X,Y,Z) = 0 (Hicks, 1969). Thus we assume that

$$(\text{div}G)(X,Y,Z) = 0 \tag{2.1}$$

where div denotes divergence.

Now differentiating (1.1) covariantly with respect to U, we get

$$(D_U G)(X,Y,Z) = a(D_U R)(X,Y,Z) + b[(D_U S)(Y,Z)X - (D_U S)(X,Z)Y] + c[g(Y,Z)(D_U Q)(X) - g(X,Z)(D_U Q)(Y)] - \frac{D_U r}{n}[\frac{a}{n-1} + b + c][g(Y,Z)X - g(X,Z)Y],$$

which on contraction gives

$$(div\, G)(X,Y,Z) = a(divR)(X,Y,Z) + b[(D_X S)(Y,Z) - (D_Y S)(X,Z)] + c[g(Y,Z)dr(X) - g(X,Z)dr(Y)] - \frac{1}{n}[\frac{a}{n-1} + b + c][g(Y,Z)\, dr(X) - g(X,Z)\, dr(Y)] \quad (2.2)$$

From (Eisenhart, 1926), we have

$$(divR)(X,Y,Z) = [(D_X S)(Y,Z) - (D_Y S)(X,Z)] \quad (2.3)$$

If LP- Sasakian manifold is an Einstein manifold, then from (1.12) and (2.3), we get

$$(divR)(X,Y,Z) = [(D_X S)(Y,Z) - (D_Y S)(X,Z)] = 0 \quad (2.4)$$

Hence in view of (2.2) and (2.4) we get

$$(div\, G)(X,Y,Z) = -(\frac{a+(n-1)b-(n-1)^2 c}{n(n-1)})[g(Y,Z)\, dr(X) - g(X,Z)dr(Y)] \quad (2.5)$$

From (2.1) and (2.5), we get

$$[g(Y,Z)dr(X) - g(X,Z)dr(Y)] = 0,$$

provided $a + (n-1)b - (n-1)^2 c \neq 0$ (2.6)

which shows that r is constant. Again if r is constant then from (2.5), we get

$$(div\, G)(X,Y,Z) = 0 \quad (2.7)$$

Hence we can state the following theorem:

Theorem (2.1): An Einstein LP-Sasakian manifold (M^n, g), $n>3$ is generalized quasi conformally conservative if and only if the scalar curvature is constant, provided $a + (n-1)b - (n-1)^2 c \neq 0$.

ϕ – generalized quasi–conformally flat LP-Sasakian manifold

Definition (3.1): A differentiable manifold (M^n, g) satisfying the condition (Cabreizo, Fernandez, Fernandez and Zhen, 1999)

$$\phi^2 G(\phi X, \phi Y, \phi Z) = 0 \quad (3.1)$$

is called ϕ–generalized quasi–conformally flat LP-Sasakian manifold. It is easy to see that

$$\phi^2 G(\phi X, \phi Y, \phi Z) = 0,$$

holds if and only if

$$g(G(\phi X, \phi Y, \phi Z), \phi W) = 0,$$

for any vector fields X, Y, Z, and W. Using (1.1), ϕ–generalized quasi–conformally flat means,

$a'R(\phi X, \phi Y, \phi Z, \phi W) = -b\,[S(\phi Y, \phi Z)\, g(\phi X, \phi W) - S(\phi X, \phi Z)\, g(\phi Y, \phi W)] - c\,[g(\phi Y, \phi Z)\, S(\phi X, \phi W) - g(\phi X, \phi Z)\, S(\phi Y, \phi W)] + \frac{r}{n}\left[\frac{a}{n-1} + b + c\right][g(\phi Y, \phi Z)\, g(\phi X, \phi W) - g(\phi X, \phi Z)\, g(\phi Y, \phi W)]$ (3.2)

Let $\{e_1, e_2, \ldots\ldots, e_{n-1}, \xi\}$ be a local orthonormal basis of vector fields in M^n. By using the fact that $\{\phi e_1, \phi e_2, \ldots\ldots, \phi e_{n-1}, \xi\}$ is also a local orthonormal basis and if we put $X = W = e_i$ in (3.2) and sum up with respect to i, then we have

$$\sum_{i=1}^{n-1} a'R(\phi e_i, \phi Y, \phi Z, \phi e_i) = -b\sum_{i}^{n-1}[S(\phi Y, \phi Z)g(\phi e_i, \phi e_i) - S(\phi e_i, \phi Z)\, g(\phi Y, \phi e_i)] - c\sum_{i}^{n-1}[g(\phi Y, \phi Z)\, S(\phi e_i, \phi e_i) - g(\phi e_i, \phi Z)\, S(\phi Y, \phi e_i)] + \frac{r}{n}\left[\frac{a}{n-1} + b + c\right] \sum_{i}^{n-1} g(\phi Y, \phi Z)\, g(\phi e_i, \phi e_i) - g(\phi e_i, \phi Z)\, g(\phi Y, \phi e_i)] \quad (3.3)$$

On LP-Sasakian manifold, we have (Ozgur, 2003)

$$\sum_{i=1}^{n-1} 'R(\phi e_i, \phi Y, \phi Z, \phi e_i) = S(\phi Y, \phi Z) + g(\phi Y, \phi Z) \quad (3.4)$$

$$\sum_{i}^{n-1} S(\phi e_i, \phi e_i) = r + n - 1 \quad (3.5)$$

$$\sum_{i}^{n-1} g(\phi e_i, \phi Z)\, S(\phi Y, \phi e_i) = S(\phi Y, \phi Z) \quad (3.6)$$

$$\sum_{i}^{n-1} g(\phi e_i, \phi Z)\, g(\phi Y, \phi e_i) = g(\phi Y, \phi Z) \quad (3.7)$$

So by virtue of (3.4) – (3.7) and then using (1.3) and (1.16), equation (3.3) takes the form,

$$S(Y,Z)\,[a + b(n-2) - c] + g(Y,Z)\,[a + (r + n - 1)\,c - \frac{r}{n}\{a + (n-1)(b + c)\}] + \eta(Y)\,\eta(Z).\,[(n-1)(a + b(n-2) - c) + a + (r + n - 1)c - \frac{r}{n}\{a + (n-1)(b + c)\}] = 0. \quad (3.8)$$

Again contracting (3.8) we get

$$r\,[a - b + c\,(2n-1)] = 0 \Rightarrow r = 0,$$

provided $a - b + c\,(2n-1) \neq 0$.

Hence we can state the following theorem:

Theorem(3.1): Let M^n be an n-dimensional (n>3) ϕ –generalized quasi–conformally flat LP-Sasakian manifold. Then M^n is of zero scalar curvature, provided

$$a - b + c\,(2n-1) \neq 0.$$

Acknowledgment: *The authors would like to thank Dr. Bhagwat Prasad, Head, Department of Mathematics, S. M. M. Town P. G. College, Ballia, for his help and encouragement.*

References

Cabrerizo, J. L., Fernandez, L. M., Fernandez, M. and Zhen, G. (1999). The structure of a class of K-contact manifolds. *Acta Math. Hungar*. **82(4)**: 331 – 340.

Eisenhart, L. P. (1926). Riemannian Geometry. Princeton Univ. Press. 82-91.

Hicks, N. J. (1969). Notes on Differential Geometry. Affiliated East West Press Pvt. Ltd. 95.

Matsumoto, K. (1989). On Lorentzian para-contact manifolds. *Bull. of Yamagata Univ. Nat. Sci.* **12 (2)**: 151- 156.

Matsumoto, K. and Mihai, I. (1988). On a certain transformation in Lorentzian para - Sasakian manifold. *Tensor, N.S.* **47**: 189-197.

Narain, D., Prakash, A. and Prasad, B. (2009). A pseudo projective curvature tensor on an LP-Sasakian manifold. *Anal. Stii. Ale. Univ. "AL.CUZA" Di Iasi. Mathematica, Tomul.* **LV (face.2)**: 275-284.

Ozgur, C. (2003). ϕ − conformally flat LP-Sasakian manifolds. *Radovi matematicki*. **12**: 99-106.

Prasad, B. (2002). A pseudo projective curvature tensor on a Riemannian manifold. *Bull. Cal. Math. Soc.* **94(3)**: 163-166.

Prasad, B., Doulo, K. and Pandey, S. N. (2011). Generalized quasi-conformal curvature tensor on a Riemannian manifold. *Tensor, N.S.* **73**: 188-197.

Yano, K. and Sawaki, S. (1972). Riemannian manifolds admitting a conformal transformation group. *J. Diff. Geometry*. **2**: 161-165.

COMPARATIVE STUDY OF LOW COST ADSORBENTS PREPARED INDIGENOUSLY FROM LOCALLY AVAILABLE BIO-WASTE FOR THE REMOVAL OF METHYLENE BLUE DYE

Daniel Kibami
Department of Chemistry, Kohima Science College (Autonomous), Jotsoma-797002, Nagaland, India
e-mail: danielkibs80@yahoo.co.in

Abstract: The removal of Methylene blue dye from aqueous solutions using *Fagopyrum esculentum* Moench *(*Buckwheat*)* and *Bambusa vulgaris* (common bamboo) as adsorbents was investigated. The effects of various experimental parameters such as effect of initial concentration, contact time and pH have been studied using batch adsorption technique. Adsorption data fitted well with all the three adsorption isotherm models. However, Frendulich isotherm displayed a better fitting model than the other two isotherms because of the higher correlation coefficient of R^2 (0.8799–0.9962) this indicates the applicability of multilayer coverage of the Methylene blue dye on the surface of adsorbent.

Keywords: Methylene blue; Batch method; Adsorption; Multilayer

Introduction

Dyeing industry effluents constitute one of the most problematic wastewaters to be treated due to their high chemical and biological oxygen demands, suspended solids, content in toxic compounds and also for colour, which are the first contaminant to be recognized by the human eye (Aksu, 2005). About 15% of the total world production of dyes is lost during the dyeing process and is released as liquid Effluents (Hollinger, 1987). The treatment of dyes in industrial wastewater presents several problems since dyes usually have a synthetic origin and complex aromatic molecular structures which make them very stable and generally difficult to be biodegraded and photodegraded (Grabowska & Gryglewicz, 2007; Gupta, 2009). Methylene blue is a thiazine (cationic) dye, which is most commonly used for coloring among all other dyes of its category. It is present in noticeable amount in industrial wastewater, which imparts blue colour. The dye causes eye burns, which may be responsible for permanent injury to the eyes of human and animals. If swallowed, the dye causes irritation to the gastrointestinal tract with symptoms of nausea, vomiting and diarrhea. It may also cause methemoglobinemia, cyanosis, convulsions, tachycardia and dyspnea, if inhaled. It is likely to cause irritation to the skin (Senthilkumar *et. al*., 2005). Many treatment techniques have been applied to a broad range of water and wastewater contaminated with dyes including physical or chemical treatment processes (Crini, 2008). These include chemical coagulation, flocculation (Aksu, 2005; Mohammad & Muttucumlutants, 2009), ozonation, oxidation, photodegradation (Elmorsi *et. al.*, 2009), ion exchange, irradiation, precipitation (Robinson *et. al.*, 2001). However, these methods are not widely used due to their high cost which requires various tools and are generally not feasible on large scale industries. In contrast, an adsorption technique is by far the most versatile and widely used. The most common adsorbent materials are: alumina silica (Josefa & Oliveira, 2003), metal hydroxides (Wu & Tseng, 2006) and activated carbon (Malik *et. al.*, 2002). It has been reported that the adsorption onto activated carbon, have proven to be the most efficient and reliable method

for the removal many pollutants, including different dyes (Aksu, 2005). Although commercial activated carbon is very effective adsorbent, its high cost requires the search for alternatives and low cost adsorbents (Pollard *et. al.,* 1992). Several low cost adsorbents have been tested for removing dyes (Garg *et. al.,*2004) including carbon from palm-tree cobs (Avom *et. al.,* 1997), plum kernels (Wu *et. al.,* 1999), cassava peel (Rajeshwarisivaraj *et. al.,* 2001), bagasse (Tsi *et. al.,* 2001), jute fiber (Senthilkumar *et. al.,* 2005), rice husks (Yalcin & Sevinc, 2000), olive stones (El-Sheikh & Newman, 2004), date pits (Girgis & El-Hendawy, 2002), fruit stones and nutshells (Aygun *et. al.,* 2003). The advantage of using agricultural by-products as raw materials for manufacturing activated carbon is that these raw materials are renewable and potentially less expensive to manufacture. Plant biomass is a natural renewable resource that can be converted into useful materials and energy (Klass, 1998). The present study is an attempt to use *Fagopyrum esculentum Moench* (FEMC) (common Buckwheat), and *Bambusa vulgaris* (common Bamboo), as non conventional low-cost adsorbent for removal of MB dye from aqueous solution. The capacity of adsorbent for adsorbate is obtained by adsorption isotherm model, which is the equilibrium relationship between adsorbent/adsorbate systems. In this study, three models (Langmuir, Freundlich and Temkin) (Otero *et. al.,* 2003; Haimour & Sayed, 1997) have been used to describe the sorption process of MB onto these absorbents.

Materials and Methods

Reagents and Apparatus

All the chemicals used are of analytical reagent grade. A stock solution of methylene blue was prepared by dissolving 1gm of methylene blue in 1000 ml of double distilled water and subsequently diluted with deionised water to the required concentration. The resultant solution contains 1000 mg/ L of methylene blue. This solution is said to be stock solution of methylene blue. The pH of the working solution was adjusted to the desired value with 0.1M HCl and 0.1M NaOH. All chemicals used were of analytical reagent grade.

The apparatus used are

1) UV-Visible Spectrophotometer (PerkinElmer, lamda-25)

2) Elico-pH Meter

Preparation, activation and surface

Characterization of different carbons

Preparation of activated carbon by indigenous method

For this study, the initial carbonization is done at bamboo mission Dimapur, Nagaland, India. In the bamboo mission, indigenous method of preparation of bamboo charcoal (taken from *Bamusa vulgaris*/ BVC) is done for commercial purpose. In this process, the whole bamboo culms are cut into a uniform size of 1 m each so that it fits into the kiln and stacking is easier. The bamboo is placed through the door at the bottom and is stacked horizontally in the kiln. The door is then closed with bricks and plastered with mud on the outside for better insulation and to prevent leakage. The feed is fired through the opening at the top of the kiln and once the feed is ignited, the opening is closed. During the initial stages of firing, the openings in the wall of the kiln are kept open to create the required draft. Initially black smoke will be emitted from the opening at upper end after which it will change to dense white fumes. Once the black smoke changes, openings are closed one by one starting from the top to

bottom. Carbonization is achieved by maintaining the temperature at 400-500°C by regulating the openings both in horizontal and vertical directions. All the openings are closed after 2 days so that air is not allowed to enter the kiln to prevent the charcoal from catching fire. Cooling is done for a day to reduce the temperature to 100°C. The biomass is removed from the opening at the bottom of the kiln and are washed, dried, and crushed and further subjected to chemical activation with 0.1N HNO_3 and 0.1N H_3PO_4. And for which the carbons were washed with double-distilled water to remove the excess acid and dried at 150°C for 12hours. All the activated carbons are chemically activated with 0.1N solution HNO_3 and 0.1 N H_3PO_4. The powdered activated carbon obtained after HNO_3 and H_3PO_4 treatment has a particle size in the range of 40-50 μm mesh. Another form of activated carbon in powder form are prepared by the pyrolysis of *Fagopyrum esculentum* Moench *(FEMC) (common Buckwheat).*The biomass were collected, washed, dried, and crushed before carbonizing in a Muffle furnace electrically heated at 600°C for 4 hours. The activated carbon prepared was cooled to room temperature and washed with deionized water until the effluent was clear in colour. Finally the synthesized carbon was dried in oven at 110 °C for 12 hour. The synthesized carbon is chemically activated with 0.1N solution HNO_3 and H_3PO_4 respectively under similar conditions to modify the chemical structure. The surface modification of carbons was also done by subjecting to liquid phase oxidation.

Adsorption Studies of methylene blue on activated carbons by Batch method

In order to understand the adsorption behavior of methylene blue dye, the effect of various experimental parameters has been investigated using batch adsorption experiments conducted at various pH values with different amounts of adsorbent. The effect of initial concentration is studied by varying methylene blue concentrations between 5- 45 mg/L. The effect of contact time was studied by varying the agitating time (range:2-240 min) at fixed optimum initial concentration of methylene blue (20mg/L) with optimum dose of adsorbents (0.25 g/L) and also the effect of pH was studied ranging from 2-10. The percentage removal of the dye and the amount of dye adsorbed were calculated by the following equations.

$$\text{Percentage removal} = 100\,\frac{(C_i - C_f)}{C_i}$$

$$\text{Amount adsorbed } (q_e) = \frac{(C_i - C_f)V}{M}$$

where C_i and C_f are the initial and final equilibrium solution concentrations of the dye (mg/ L), V is the volume of the solution (L) and M is the mass of the activated carbon (g). The data obtained have been analyzed for adsorption isotherms models.

Results and discussion

Effect of initial concentration

The effect of initial concentration on the adsorption of methylene blue was studied by varying the initial dye concentration between 5- 45 mg/L in 100 ml of methylene blue dye solution and adding 1 g of adsorbent and contact time of 120 mins. The effect of the initial dye concentration depends on the immediate relation between the dye concentration and the available binding sites on an adsorbent surface (Salleh *et. al.*, 2011). Fig.1.1. shows the effect of initial dye concentration with different adsorbents [BVC (HNO_3), BVC (H_3PO_4), FEMC (HNO_3) and

FEMC (H_3PO_4)]. The relevant data shows that the amount adsorbed exponentially increases while the percentage removal exponentially decreases with the increase in initial concentration of the methylene blue. Generally the percentage of dye removal decreases with an increase in initial dye concentration, which may be due to the saturation of adsorption sites on the adsorbent surface (Eren & Acar, 2006). At low concentration, there will be unoccupied active sites on the adsorbent surface, and when the initial dye concentration increases, the active sites required for adsorption of the dye molecules will disappear (Kannan & Sundram, 2001). However, the increase in the initial dye concentration will cause an increase in the loading capacity of the adsorbent and this may be due to the high driving force for mass at a high initial dye concentration (Gouamid *et. al.*, 2006). In other words, the residual concentration of dye molecules will be higher for higher initial dye concentrations. The variation of percent removal of methylene blue with increasing Initial concentration is shown in Fig 1.1.

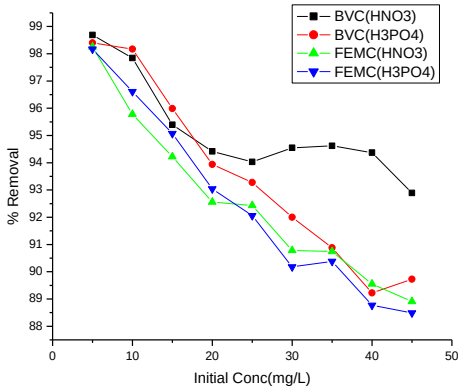

Fig 1.1: Variation of percent removal of methylene blue with increasing initial concentration.

Adsorption Isotherm

An adsorption isotherm gives the relationship between the amount of a substance adsorbed at constant temperature and its concentration in the equilibrium solution (Langmuir, 1918). Langmuir, Freundlich and Temkin adsorption isotherm models are employed in this study to describe the experimental adsorption isotherm (Hameed *et. al.*,2007).

Langmuir adsorption is based on the fact that maximum adsorption corresponds to a saturated monolayer of solute molecules on the adsorbent surface. The linear form of the Langmuir equation can be represented by

$$\frac{C_e}{q_e} = \frac{1}{b}Q_0 + \frac{C_e}{Q_0}$$

Where q_e is the amount of methylene blue adsorbed (mg/ g) and C_e is the equilibrium concentration of methylene blue in the bulk solution (mg/ L) while Q_0 is the monolayer adsorption capacity (mg/ g) and b is the Langmuir constant related to energy adsorption capacity. The constants Q_0 and b can be calculated from slope and intercept of the plot C_e/q_e vrs C_e (Areco & Afonso, 2010). Freundlich isotherm is an empirical equation describing the heterogeneous adsorption and assumes that different sites with several adsorption energies are involved (Freundlich & Helle, 1939). The linear form of the Freundlich equation is shown below.

$$Log\ q_e = log\ k + \frac{1}{n}\ log\ C_e$$

The slope 1/n gives adsorption capacity and intercept log K gives adsorption intensity from straight portion of the linear plot obtained by plotting log q_e versus log C_e. Temkin isotherm model predicts a uniform distribution of

binding energies over the population of surface binding adsorption (Temkin & Pyzhev, 1940).

The Temkin isotherm is applied in the following form

$$q_e = \frac{RT}{b_T} \ln (A_T.C_e)$$

The linear form of Temkin equation is

$$q_e = \frac{RT}{b_T} \ln A_T + \frac{RT}{b_T} \ln C_e$$

$$q_e = \beta \ln\alpha + \beta \ln C_e$$

Where, $\beta = \frac{RT}{b_T}$; $\alpha = A_T$

T is the absolute temperature in Kelvin, R is the universal gas constant, 8.314 J/mol K, b_T is the Temkin constant related to heat of sorption (J/mg) and A_T the equilibrium binding constant corresponding to the maximum binding energy (L/g) The Temkin constants A_T and b_T are calculated from the slopes and intercepts of q_e vs ln C_e.

Table 1: Langmuir adsorption isotherm model showing constant values.

Adsorbent	R^2	q_m	k_L	a_L
Units		(mmol/g)	(L/g)	(L/mg)
BVC (HNO_3)	0.9607	1.7461	9.5602	5.4751
BVC (H_3PO_4)	0.9590	1.7352	6.9735	4.0188
FEMC(HNO_3)	0.9397	1.5391	6.8768	4.4681
FEMC(H_3PO_4)	0.8591	1.4092	5.1466	3.6521

Table 2: Frendulich adsorption isotherm model showing the constant values.

Adsorbent	R^2	Log K	1/n	K
Units				
BVC (HNO_3)	0.9962	0.3517	0.5666	2.2475
BVC (H_3PO_4)	0.9781	0.2456	0.4985	1.7603
FEMC(HNO_3)	0.9334	0.1681	0.5323	1.4726
FEMC(H_3PO_4)	0.8799	0.1471	0.5102	1.4034

Table 3: Temkin adsorption isotherm model showing the constant values.

Adsorbent	R^2	b_T	Bln(A)	A_T
Units		(J/mg)		(L/g)
BVC (HNO_3)	0.9962	0.3517	0.5666	2.2475
BVC (H_3PO_4)	0.9781	0.2456	0.4985	1.7603
FEMC(HNO_3)	0.9334	0.1681	0.5323	1.4726
FEMC(H_3PO_4)	0.8799	0.1471	0.5102	1.4034

Effect of contact time

The effect of contact time on the removal of methylene blue dye was studied by varying the agitating time (range: 2-240 min) at fixed optimum initial concentration of methylene blue (20mg/L) with a dose of adsorbents (0.25 g/L). The contact time plot shows the removal of methylene blue is rapid in early stages but it gradually slows down until it reaches the equilibrium. The initial rate of adsorption was greater because the diffusion of dye molecules through the solution to the surface adsorbents is effected by the dye concentration.Once equilibrium was attained, the percentage sorption did not change with further increases of time. The equilibrium was attained after shaking for 240 min. The decrease in the extent of removal of methylene blue after 240 min of contact time in some

cases may be due to the desorption process (Franca *et. al.,* 2009). The relation between contact time and percent removal of methylene blue is shown in the Fig 1.2.

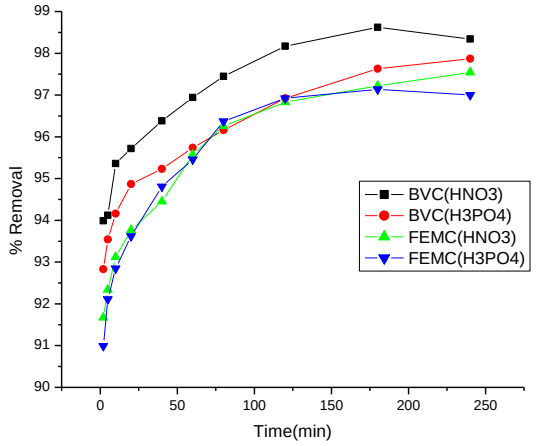

Fig 1.2: Effect of Contact time on percent removal of methylene blue dye.

Effect of pH

The pH of a medium controls the magnitude of electrostatic charges which are imparted by the ionized dye molecules. As a result, the rate of adsorption will vary with the pH of an aqueous medium (Senthilkumar *et. al.,* 2005). The effects of initial pH on dye solution were investigated by varying the pH from 2 to 10 and using initial dye concentration of 20 mg/L with contact time of 120 mins. At pH 2 the removal was minimum but it increased along with increasing initial pH of dye solution. The result in Fig. 1.11 shows that, the maximum adsorption was observed at pH 9 for BVC (HNO_3) and BVC (H_3PO_4). At pH 9 the dye removal percentage was 98.43% and 98.24% respectively. The maximum adsorption was observed for FEMC (HNO_3) when pH rises up to 10. However in case of FEMC (H_3PO_4) the adsorption capacity decreased when the pH was increased from 8. This can be attributed due to the negative charge on the surface that is very much reduced due to the excess protons in solution when compared to other adsorbents. The methylene blue adsorption usually increases as the pH is increased. Lower adsorption of MB at acidic pH is probably due to the presence of excess H^+ ions competing with the cation groups on the dye for adsorption sites. At higher pH, the surface of activated carbon particles may get negatively charged, which enhances the adsorption of positively charged dye cations through electrostatic forces of attraction (Onal *et. al.*,2006; Hameed *et. al.*, 2008). Such observations were also reported by B.H. Hameed and S. Cengiz (Hameed & Khaiary, 2008; Cengiz & Cavas, 2008).

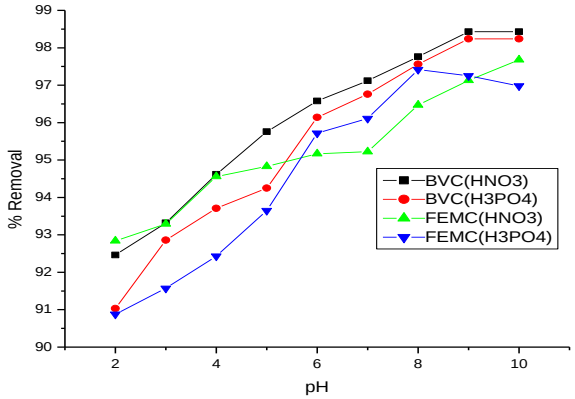

Fig 1.3: Effect of pH on percent removal of methylene blue dye.

Conclusions

Adsorption studies of methylene blue on activated carbons was studied where effect of initial concentration, effect of contact time and effect of pH were the parameters considered to determine the adsorption efficiency of the carbon samples. The results of the percentage removal of methylene blue

dye increased with the increase of contact time and pH. On the contrary, the percentage of removal has decreased with the increase in initial concentration of the standard methylene blue solution. The basic medium highly influences the maximum removal of methylene blue which may due to the preference of the dye cations for basic sites. The equilibrium data have been analyzed using Langmuir, Frendulich and Temkin isotherms. The adsorption data obeyed all the three isotherms up to some extent. However out of three isotherm models studied for this adsorbent-adsorbate system, Frendulich isotherm with high R^2 (0.8799–0.9962) was the most suitable equation to describe the adsorption indicating a multilayer adsorption with heterogeneous distribution of active sites on the adsorbent. Thus these activated carbons can be effectively used for the removal of methylene blue dye. Among the four low-cost adsorbents under consideration, the order of adsorption capacity of the various adsorbents is as follows: BVC (HNO_3) > BVC (H_3PO_4) > FEMC (HNO_3) > FEMC (H_3PO_4). This indicates the chemical activation by HNO_3 is more effective than H_3PO_4 activation for a given biowaste material. Among the adsorbents which were indigenously prepared BVC (HNO_3) possesses the highest or the maximum adsorption capacity. Hence it is the best and the most effective adsorbent in the removal of methylene blue content in water. The suggested adsorbent materials are very cheap and are abundantly available. Because of their economic viability, these low cost adsorbents can be used in the process of eliminating the undesirable and unwanted ingredients in water.

References

Aksu. Z. (2005). *Process Biochemistry*. **40(3-4)**: 997.

Areco, M. M. and Afonso, M. S. (2010). *Biointerfaces*. **81**: 620.

Avom, J., Mbadcam, J. K., Noubactep, C. and Germain, P. (1997) *Carbon*. **35**: 365.

Aygun, A ., Yenisoy Karakas, S. and Duman, I. (2003). *Microporous & Mesoporous materials*. **66**:189.

Cengiz, S. and Cavas, L. (2008). *Bioresource Technology*. **99**: 2357.

Crini, G. (2008). *Dyes and Pigments*. **77(2)**: 415.

Elmorsi, T. M., Riyad, Y. M., Mohamed, Z. H. and Abd El Bary, H. M. (2010). *Journal of Hazardous Materials*. **174(1-3)**: 352.

El-Sheikh, A. H. and Newman, A. P. (2004). *Journal of Analytical and Application Pyrolysis*. **71**: 151.

Eren, Z. and Acar, F. N. (2006). *Desalination*. **194**:1.

Feng-Chin Wu and Ru-Ling Tseng (2006). *Journal of Colloid and Interface Science*. **294**: 21.

Franca, A. S., Oliveira, L. S. and Ferreira, M. E. (2009). *Desalination*. **249**: 267.

Freundlich, H. and Helle, W. J. (1939). *Journal of American Chemical society*. **61**: 2.

Garg, V. K., Amita, M., Kumar, R. and Gupta, R. (2004). *Dyes and Pigments*. **63(3)**: 243.

Girgis, B. S. and El-Hendawy, A. A. (2002). *Microporous & Mesoporous Materials*. **52**:105.

Gouamid, M., Ouahrani, M. R. and Bensaci, M. B. (2006). *Desalination*. **194**: 259.

Gupta, V. (2009). *Journal of Environmental Management*. **90(8)**: 2313.

Haimour, N. and Sayed, S. (1997). *Natural and Engineering Science.* **24**: 215.

Hameed, B. H., Din, A. T. M. and Ahmad. A. L. (2007). *Journal of Hazardous Materials*. **22,141(3)**: 819.

Hameed, B. H., Mahmoud, D. K. and Ahmad, A. L. (2008). *Journal of Hazardous materials*.**158**: 65.

Hameed, B. H. and Khaiary, M. I. E. (2008). *Journal of Hazardous materials*. **154**: 639.

Josefa, S. Y. M. and De Oliveira, E. (2003). *Advance Environmental Research*. **7**: 263.

Kannan, N. and Sundram. M. M. (2001). *Dyes and pigments*.**51**: 25.

Klass, D. L. (1998). Biomass for Renewable Energy, Fuels, and Chemicals, Academic Press, San Diego, CA.

Langmuir, I. (1918). *The Research Laboratory of the General Electric Journal of American Chemical society*. **40**: 1361.

Lorenc-Grabowska, E. and Gryglewicz, G. (2007). *Dyes Pigments*. **74(1)**: 34.

Malik, D. J., Strelko Jr, V., Streat, M. and Puziy, A. M.(2002). *Water Research*. **36**: 1527.

Mohammad, M. E. and Muttucumlutants, S. (2009). *Journal of Environmental Management*. **90(5)**:1663.

Önal, Y., Akmil-Basar, C., Eren, D., SarIcI-Özdemir, C. and Depci, T. (2006). *Journal of Hazardous materials*.**128(2-3)**:194.

Otero, M., Rozada, F., Garcoia, A. and Moran. (2003). *Chemical Engineering Journal*. **15**: 59.

Pollard, S. J. T., Fowler, G. D., Sollars, C. J. and Perry, R. (1992). *Science of the Total Environment*. **116(1-2)**: 31.

Senthilkumar, S., Porkodi, K. and Vidyalakshmi, R. (2005). *Journal of Photochem. Photo-biol*. 170-225.

Rajeshwarisivaraj, S., Sivakumar, P. Senthilkumar, V. and Subburam. (2001). *Bioresour. Technol*. **80**: 233.

Robinson, T., McMullan, G., Marchant, R. and Nigam, P. (2001). *Bioresource Technology*. **77(3)**: 247.

Salleh, M. A. M., Mahmoud, D. K., Karim, W. A. W. A. and Idris, A. (2011). *Desalination*. **280**:1.

Senthilkumaar, S., Varadarajan, P. R. Porkodi, K. and Subbhuraam, C.V. (2005). *Journal of Colloid & Interface Science*. **284**: 78.

Senthilkumar, S., Varadarajan, P. R., Porkodi, Temkin, M. J. and Pyzhev, V. (1940). *Acta Physiochim.Urss*. **12**: 217.

Tsai, W. T., Chang, C.Y., Lin, M. C., Chien, S. F., Sun, H. F. and Hsieh, M. F. (2001). *Chemosphere*. **45**: 51.

Wu, F. C., Tseng, R. L. and Juang, R. S. (1999). *Journal of Hazardous Materials*. **69**: 287.

Yalcin, N. and Sevinc, V. (2000). *Carbon.* **38**: 1943.

Zolllinger, H. (1987). VCH publisher, New York. 92.

CLOSED INJECTIVE MODULES-AN OVERVIEW

*J. R. Yimchunger and **M. K. Patel

*Department of Mathematics, Kohima Science College (Autonomous), Jotsoma-797002, Nagaland, India
**Department of Mathematics, National Institute of Technology, Nagaland, Dimapur-797103, India
e-mail: *janeroselineyim@gmail.com, **mkpitb@gmail.com

Abstract: This overview mostly encompasses basic facts and results on generalizations of c-injective (closed injective) modules developed by the authors- Dinh (2005), Chaturvedi *et. al.* (2010), Kumar *et. al.* (2012) and Baupradist *et. al.* (2012). Also, the motivation for this work is based, to some extent, on ideas and concepts developed by the authors- Mohamed *et. al.* (1990), Wisbauer (1991), Lam (1998) and Smith & Tercan (1992). In this article, we provide important results and examples to understand the concepts of M-c-injective, quasi-c-injective and pseudo-c-injective modules, and also to generate interest for further research on related concepts discussed here.

Keywords: M-c-injective module, quasi-c-injective module and pseudo-c-injective module.

Introduction

Throughout this paper, all rings are associative with unity, and all modules are unitary right modules. Given two modules M and N, N is called **M-injective** if for every submodule A of M, any homomorphism $f : \mathrm{A} \to \mathrm{N}$ can be extended to a homomorphism $g : \mathrm{M} \to \mathrm{N}$. A module N is called **injective** if it is M-injective for every R-module M. N is called **quasi-injective** if N is N-injective. N is **M-pseudo injective** if for every submodule A of M, any monomorphism $f : \mathrm{A} \to \mathrm{N}$ can be extended to a homomorphism $g : \mathrm{M} \to \mathrm{N}$. N is called **pseudo-injective** if N is N-pseudo injective. Two modules A and B are called mutually (pseudo)injective if A is B (pseudo) injective and B is A (pseudo) injective.

Consider the following conditions for a module M:

(C_1) Every submodule of M is essential in a direct summand of M.

(C_2) If a submodule A of M is isomorphic to a direct summand of M, then A is itself a direct summand of M.

(C_3) If A and B are direct summands of M such that $\mathrm{A} \cap \mathrm{B} = 0$, then $\mathrm{A} \oplus \mathrm{B}$ is also a direct summand of M.

M is called a **CS** module or an **extending** module if M satisfies (C_1). M is called **continuous** if it satisfies (C_1) and (C_2). M is called **quasi-continuous** if it satisfies (C_1) and (C_3).

Quasi-injective and pseudo-injective modules

Proposition 1.1. [6, Proposition 2.1]

(i) If N is M-pseudo injective, then any monomorphism $f : \mathrm{N} \to \mathrm{M}$ splits.

(ii) If N is M-pseudo-injective, then N is A-pseudo-injective for any submodule A of M.

(iii) Every direct summand of an M-pseudo-injective module is also M-pseudo-injective.

Theorem 1.2. [6, Theorem 2.2] If $M_1 \oplus M_2$ is pseudo-injective, then M_1 and M_2 are mutually injective.

Proposition 1.3. [6, Corollary 2.4] For any integer $n \geq 2$, M^n is pseudo-injective if and only if M is quasi-injective.

Proposition 1.4. [6, Theorem 2.6] Any pseudo-injective module satisfies (C_2).

Corollary 1.5. A pseudo-injective CS module is continuous.

Theorem 1.6. [15, Theorem 2.1] For a commutative ring R, the following conditions are equivalent:

(i) The direct sum of two pseudo injective modules is pseudo injective.
(ii) Every pseudo injective module is injective,
(iii) R is semi-simple.

Corollary 1.7. For a commutative ring R, the following conditions are equivalent:

(i) The direct sum of two quasi injective modules is quasi injective.
(ii) Every quasi injective module is injective.
(iii) R is semi-simple.

Theorem 1.8. [7, Corollary 1] A module M is quasi-injective if and only if $M \oplus M$ is pseudo-injective.

M-c-injective and quasi-c- injective modules

A submodule N of an R-module M is said to be an **essential** submodule of M if $N \cap A \neq 0$ for all non-zero submodule A of M. A submodule K of a module M is said to be a **closed** submodule of M if K has no proper essential extension inside M. A submodule H of M is called a **complement** of a submodule N of M, if H is maximal in the collection of submodules G of M such that $G \cap N = 0$. A module N is called **M-c-injective** if for every closed submodule A of M, any homomorphism $f : A \to N$ can be extended to a homomorphism $g : M \to N$. A module M is called **quasi-c- injective** if it is M-c-injective.

The following implications hold:

Injective $\Rightarrow$ quasi-injective $\Rightarrow$ continuous $\Rightarrow$ quasi-continuous $\Rightarrow$ CS $\Rightarrow$ quasi-c-injective.

But none of the converses hold in general.

Remark 2.1. If M_2 is an M_1-injective module, then M_2 is also an M_1-c-injective module. The following example shows that the converse is not true in general:

Let $R = \begin{pmatrix} F & F \\ 0 & F \end{pmatrix}$, where F is a field; $M_1 = \begin{pmatrix} F & F \\ 0 & 0 \end{pmatrix}$ and $M_2 = \begin{pmatrix} 0 & 0 \\ 0 & F \end{pmatrix}$.

Then it is clear that M_2 is not M_1-injective. The only submodules of M_1 are $0, M_1$ and $\begin{pmatrix} 0 & F \\ 0 & 0 \end{pmatrix}$, where $\begin{pmatrix} 0 & F \\ 0 & 0 \end{pmatrix}$ is essential in M_1. So, the closed submodules of M_1 are 0 and M_1. Hence, M_2 is M_1-c-injective.

Proposition 2.2. [8, Proposition 2.15]

(i) Let X, Y, and M be R-modules where $X \cong Y$. If X is M-c-injective, then Y is also M-c-injective.

(ii) Let X, Y, and M be R-modules where $X \cong Y$. If M is Y-c-injective, then M is also X-c-injective.

Proposition 2.3. [8, Proposition 2.1] Let M and A be two R-modules. Then the following statements are equivalent:

(i) M is A-c-injective.
(ii) M is B-c-injective, for every closed submodule B of A.

(iii) N is A-c-injective, for every direct summand N of M.
(iv) N is B-c-injective, for every direct summand N of M and every closed submodule B of A.

Proposition 2.4. Any direct summand of a quasi-c-injective module is also quasi-c-injective.

Proposition 2.5. An R-module M is quasi-c-injective if and only if M is A-c-injective for every closed submodule A of M.

Proposition 2.6. [8, Proposition 2.3] An R-module M is injective if and only if M is N-c-injective for all R-modules N.

Pseudo-c-injective Modules

A right R-module N is called **M-pseudo-c- injective** if for every closed submodule A of M, any monomorphism $f: A \to N$ can be extended to a homomorphism $g: M \to N$. If M is M-pseudo-c-injective then M is called **pseudo-c-injective** module.
The following example shows that not every M-pseudo-c-injective module is M-pseudo injective:
Let $R = \begin{pmatrix} F & F \\ 0 & F \end{pmatrix}$, where F is a field; $M = \begin{pmatrix} F & F \\ 0 & 0 \end{pmatrix}$ and $N = \begin{pmatrix} 0 & 0 \\ 0 & F \end{pmatrix}$, where M and N are right R-modules. Then N is M-pseudo-c-injective but not M-pseudo-injective.
Any monomorphism $f: N \to M$, where N is a closed submodule of M is said to be a **c-monomorphism**.

Proposition 3.1. [9, Proposition 2.4] If N is an M-pseudo-c-injective module, then any c-monomorphism $f: N \to M$ splits.

Proposition 3.2. If N is an M-pseudo-c-injective module, then N is L-pseudo-c-injective for any closed submodule L of M.

Proposition 3.3. [9, Proposition 2.7] Every direct summand of a pseudo-c-injective module is also pseudo-c-injective.

Proposition 3.4. [9, Proposition 2.8] If M is a pseudo-c-injective module, then every fully invariant closed submodule of M is also pseudo-c-injective.

Proposition 3.5. [9, Proposition 2.13] If $M_1 \oplus M_2$ is a pseudo-c-injective module, then M_1 and M_2 are mutually c-injective.

Remark 3.6. Every extending module is c-injective. Also, every c-injective module is pseudo-c-injective. Thus it follows that every extending module is pseudo-c-injective but the converse need not be true as shown by the following example: The $\mathbf{Z}$-module $Q \oplus \mathbf{Z}/p\mathbf{Z}$ for any prime *p*, is pseudo-c-injective but not extending (Smith and Tercan, 1992).

Theorem 3.7. [9, Theorem 2.17] For a commutative ring R, the following statements are equivalent:
(i) The direct sum of two pseudo-c-injective R-modules is also pseudo-c-injective;
(ii) Every pseudo-c-injective module is injective;
(iii) R is semi-simple Artinian.

Corollary 3.8. For a commutative ring R, the following statements are equivalent:
(i) The direct sum of two c-injective R-modules is also c-injective;
(ii) Every c-injective module is injective;
(iii) R is semi-simple Artinian.

A submodule K of M is called **fully invariant** if $f(K) \subseteq K \ \forall \ f \in End_R(M)$,

i.e., K is invariant under every endomorphism of M. A module M is called a **duo** module if every submodule of M is fully invariant. A module M is said to have the **summand intersection property (SIP)** if the intersection of two direct summands of M is also a direct summand of M.

Proposition 3.9. [9, Proposition 2.24] A duo pseudo-c-injective module M has the SIP.

Proposition 3.10. Let X, Y and M be R-modules where $X \cong Y$. If X is M-pseudo-c-injective, then Y is also M-pseudo-c-injective.

Proposition 3.11. Let M be a right R-module and X be a closed submodule of M. If X is M-pseudo-c-injective, then X is a direct summand of M.

Proposition 3.12. [10, Theorem 2.6] Let M and N be right modules. If N is M-pseudo-c-injective, then A is a B-pseudo-c-injective module, where A is a direct summand of N and B is a direct summand of M.

Definition 3.13. A right R-module M is called **co-Hopfian** (**Hopfian**) if every injective (surjective) endomorphism $f : M \to M$ is an automorphism. A right R-module is called **directly finite** if it is not isomorphic to a proper direct summand of M.

Lemma 3.14. [2, Proposition 1.25] A right R-module M is directly finite if and only if $f \circ g = I$ implies $g \circ f = I$ for all $f, g \in S = End_R(M)$ where *I* is the identity map from *M* to *M*.

Proposition 3.15. [10, Proposition 2.17] A pseudo-c-injective module M is directly finite if and only if it is co-Hopfian.

Corollary 3.16. [10, Proposition 2.18] If M is an indecomposable pseudo-c-injective module then M is co-Hopfian.

Corollary 3.17. If a module M is pseudo-c-injective and Hopfian, then M is co-Hopfian.

Corollary 3.18. If a module M is c-injective and Hopfian, then M is co-Hopfian.

Acknowledgement*: The first author is thankful to her supervisor Dr. Manoj Kumar Patel for his suggestions and helpful comments.*

References

Anderson, F. W. and Fuller, K. R. (1974). Rings and Categories of Modules, Springer-verlag, New York.

Baupradist, S., Sitthiwirattham, T. and Asawasamrit, S. (2012). On generalizations of pseudo-injectivity, *Int. J. Math. Anal.* **6(12)**: 555-562.

Byrd, K. A. (1972). Rings whose quasi-injective modules are injective. *Proc. Amer. Math. Soc.* **33(2)**.

Chaturvedi, A. K., Pandeya, B. M., Tripathi, A. M. and Mishra, O. P. (2010). On M-c-Injective and Self-c-Injective Modules, *Asian-European J. of Math*. **3(3)**: 387-393.

Dinh, H. Q. (2005). A note on pseudo-injective modules. *Comm. Algebra*. **33**: 361-369.

Dung, N. V., Huynh, D. V., Smith, P. F., Wisbauer, R. (1994). Extending Modules, Pitman, London.

Haghany, A. and Vedadi, M. R. (2001). Modules whose injective endomorphisms are essential. *J. Algebra*. **243**: 765-779.

Jain, S. K. and Singh, S. (1975). Quasi-injective and pseudo-injective modules. *Canad. Math. Bull*. **18**: 359–366.

Koehler, A. (1971). Quasi-projective and Quasi-injective modules, *Pacific J. Math.* **36(3)**.

Kumar, V., Gupta, A. J., Pandeya, B. M. and Patel, M. K. (2012). M-c-pseudo injective modules, *East-West J. of Math*. **14(1)**: 67-75.

Lam, T. Y. (1998). Lectures on Modules and Rings, Graduate Texts in Mathematics. Springer- Verlag, New York/ Berlin, **139**.

Mermut, E., Clara, C. S. and Smith, P. F. (2009). Injectivity relative to closed submodules. *J. Algebra*. **321**: 548–557.

Mohamed, S. H. and Müller, B. J. (1990). Continuous and Discrete Modules. *London Math. Soc*. 147.

Singh, S. and Jain, S. K. (1967). On pseudo injective modules and self injective rings. *J. Math. Sciences*. **2(1)**.

Smith, P. F. and Tercan, A. (1992). Continuous and Quasi-continuous modules. *Houston J. Math*. 339-347.

Teply, M. L. (1975). Pseudo-injective modules which are not quasi-injective. *Proc. Amer. Math. Soc*. **49(2)**.

Tiwary, A. K. and Pandeya, B. M. (1978). Pseudo projective and pseudo injective modules, *Indian J. Pure and Applied Math*. **9(9)**: 941-949.

Wisbauer, R. (1991). Foundations of Module and Ring Theory, Gordon and Breach London, Tokyo.

TITLE: THERMAL DEGRADATION KINETIC STUDIES OF TETRAPROPYLAMMONIUM TRIBROMIDE (TPATB) - A ROUTE TO REACTIVITY ASSESSMENT FOR SOLVENT-FREE REACTIONS

Neivotsonuo B. Kuotsu
Department of Chemistry, Kohima Science College (Autonomous), Jotsoma-797002, Nagaland, India.
e-mail: solo_berna@yahoo.com

Abstract: Tetraproylammonium tribromide (TPATB) is an important alternative to the hazardous reagent bromine because of their efficiency to various organic transformations, especially bromination reactions. In the context of green chemistry, development of solvent-free reaction protocols is much needed which will ultimately cut down pollution to certain extent. In order to assess the behaviour of these tribromide in solvent-free reactions at elevated temperatures, thermogravimetric studies came in as a useful tool. Thus, the kinetics of the thermal degradation of TPATB was studied through thermogravimetric analysis. Non-isothermal multiple heating rate model free methods namely Ozawa-Flynn-Wall and Kissinger methods are used to calculate degradation activation energy of TPATB. The reaction mechanism based on activation energy calculation at different conversions has been proposed.

Keywords: Tetrapropylammonium tribromide, Thermal analysis, Bromination Solvent-free, Environmentally benign**.**

Introduction

Acknowledging the importance of bromo-organic compounds (Anastas *et. al.*, 2000; 2007) and the need for environmentally benign brominating reagents, substantial developments have been made through the synthesis and use of quaternary ammonium tribromides (QATBs) as alternatives of bromine (Chaudhuri *et. al.,* 2004; Alimenla *et. al.,* 2014). Among the numerous tribromides that have been synthesized so far tretapropyl ammonium tribromide (TPATB), have been found to be useful for a number of different types of reactions, including solvent-free brominations conducted at elevated temperature and under microwave conditions (Chaudhuri *et. al.*, 2004; Kar *et. al.,* 2003). Ability for any reagent to performed at high temperature greatly broadens the scope of the reagent for other solvent-free reactions and thereby it becomes important to understand their degradation pattern at elevated temperature. It has been observed that in the case of QATBs, other than a brief study on CTMATB (Bose *et. al.,* 2001) there seems to be no report on thermal analysis.

Thermogravimetric analysis (TGA) has been used widely to estimate the kinetic parameters of degradation processes, such as activation energy (Ea), reaction orders (n) and the Arrhenius pre-exponential factor(A) (Kissinger, 1957; Arora *et. al.,* 2011). Kinetic data obtained from TGA are very useful to understand the thermal degradation processes and mechanisms, and also may be used as input parameters for a model of thermal degradation reaction. Acknowledging the importance of such kind of a study, tetrapropylammonium tribromide (TPATB) have been taken as candidates for estimating the kinetic parameters of degradation processes such as activation energies(Ea) and the Arrhenius pre-exponential factor(A) (Badia *et. al.,* 2010; Hamcuic *et. al.,* 2007; Wang *et. al.,*2011; Fraga and Niinez, 2001). Accordingly, this

paper deals with the thermal and kinetic study of TPATB using simultaneous thermal analysis by the Kissinger (Kissinger, 1957) and Flyn-Wall-Ozawa methods (Wang *et. al.*,2011; Fraga and NiInez, 2001). Activation energy can be calculated using Eq. (1) with Kissinger method without knowing the solid-state degradation reaction mechanism (Mehran *et. al.*,, 2015; Katarzyna *et. al.*, 2011).

$$\ln\left(\frac{\beta}{T_{max}^2}\right) = \ln\frac{AR}{Ea} + \ln(n[1-\alpha_{max}^{n-1}]) - \left(\frac{E}{RT_{max}}\right) \ldots\ldots (1)$$

where β is heating rate, T_{max} is temperature related to maximum reaction rate, A is the pre-exponential factor , α_{max} is the maximum degradation fraction, n is reaction order. Plotting $\ln(\beta/T^2_{max})$ versus $(1000/T_{max})$ gives activation energy from slope.

The Kissinger plot thus says that for a given DSC curve with the heating rate β, one observes the maximum reaction rate at the peak temperature T_p; for a set of DSC curves with different heating rates, one can plot the quantity of $\ln(\beta/T_p^2)$ against $1/T_p$ to obtain the Kissinger plot. From the slope of the Kissinger plot, one in turn obtains the activation energy, E_a; further, from the intercept one obtains the pre-exponential factor, *A*, as well.

The Flyn-Wall-Ozawa method is an integral method that can be used to determined the activation energy without the knowledge of reaction mechanism (Burnham, 2000; Askari *et. al.*,2015). This is based on the information that the pre-exponential factor (A) and activation energy (E_a) do not depend on degradation fraction, but they depend on the temperature. This method uses equation (2) as:

$$\log(\alpha) = \log\left(\frac{AEa}{R}\right) - \log\beta + \log P\left(\frac{E}{RT}\right) \ldots\ldots\ldots (2)$$

When Doyle approximation is used, then equation 2 can be obtained.

$$\log\beta = \log\left(\frac{AEa}{R}\right) - \log g(\alpha) - 2.314 - 0.4567\left(\frac{E}{RT}\right) \ldots\ldots (3)$$

where β is the heating rate and g(α) is the conversion temperature. The plot of log β versus 1000/T should be linear with the slope E_a/R from which E_a can be calculated.

Experimental

Synthesis of Tetrapropylammonium Tribromide (TPATB)

0.057g (0.53mmol) sodium carbonate Na_2CO_3 was added to 50% H_2O_2 (10 ml; 47 mmol) and the mixture was stirred at room temperature for about 5 minutes until Na_2CO_3 completely dissolved and the mixture became a clear colourless solution. To this was added a solution of 5 g (18.79 mmol) tetrapropylammonium bromide (TPAB), and 3.7 g (31.09mmol) potassium bromide (KBr), both dissolved together in 50 ml of water. To the resultant reaction mixture, 50 ml of 2 M H_2SO_4 was added in small portions, upon which yellow precipitate appeared immediately. The mixture was allowed to be stirred for further 1 h whereby a bright yellow coloured compound precipitated out completely. The compound was filtered under suction using Whatman-40 filter paper and dried in vacuum desiccator using self-indicating coarse silica gel. It was further recrystallized in acetonitrile, isolated by suction filtration and dried in vacuo yielding 7 g (88 %) of the pure compound.

Thermogravimetric Analysis

Thermogravimetric(TG) experiments were conducted on a Perkin Elmer STA - 6000 (Simultaneous Thermal Analyser). 12

mg of sample was taken in the crucible and heated from 30 to 300^{0}C at a heating rate of 5, 10, 15, 20 ^{0}C/min, in nitrogen atmosphere, at a purge rate of 20 mL/min.

Data processing and activation energy calculation

TG curves were obtained from TG Analyzer. The curves were then analysed by using pyris software from TG Analyzer and data was used in MS Excel software to calculate activation energy (Ea) by the method of least square. Activation energy of samples was calculated by model free iso-conversional methods. Kissinger method was used in calculating activation energy at different heating rate (β) which is given by the equation (4) as:

$$\ln\left(\frac{\beta}{T_{max}^2}\right) = \ln\frac{AR}{Ea} + \ln(n[1-\alpha_{max}^{n-1}]) - \left(\frac{E}{RTmax}\right) \ldots\ldots 4$$

where β is heating rate, T_{max} is temperature related to maximum reaction rate, A is pre-exponential factor, α_{max} is maximum degradation fraction, n is reaction order. Plotting ln (β/T^2_{max}) versus ($1000/T_{max}$) gives activation energy from slope. Flyn-Wall-Ozawa method was also used to determine the activation energy at a fixed conversion with the slope of such a line being -0.4567 Ea/ RT.

Results and Discussion

In thermogravimetric analysis, the mass of a sample in a controlled atmosphere is recorded continuously as a function of temperature / time. A plot of mass or mass percent as a function of time is called a thermogram or a thermal decomposition curve (Earnest, 1984).

TG curves were obtained for TPATB at different heating rates in nitrogen atmosphere as shown in figure 1.

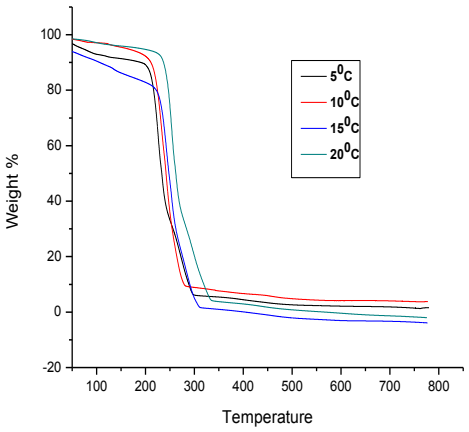

Figure 1.TG curve of TPATB at 5,10,15,20^{0}C

It can be observed that the shapes of the TG curves are quite similar, shifting towards higher temperatures at higher heating rates. This is probably due to the heat transfer lag with increased heating rate.

The initial decomposition temperature of TPATB occurs around 179^{0}C as shown in figure 2. The main decomposition of TPATB occurs around 307^{0}C with a percentage mass of 3% remaining as unburned.

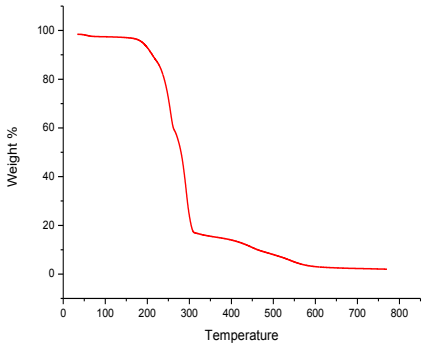

Figure 2.*TG curve of* ***TPATB*** *at 10^{0}C/min*

Degradation activation energy of TPATB

From the study of degradation of activation energies, we can predict the stability of any compound, hence these energies were obtained for the quaternary ammonium tribromide by applying the Kissinger method of calculation. Accordingly, activation energies for TPATB was calculated using Kissinger method at varying heating rates (β) and are given in Table 1. The T_{max} values given in the table below are converted into Kelvin scale of temperature for calculations.

Table 1. Calculation of activation energies for decomposition of **TPATB** at varying degree of conversions

β	ln β	T_{max}	T_{max} K	T_{max}sq	β/T_{max}sq	lnβ/T_{max}sq	1000/T_{max}
278	5.627	229.3	502.3	252305	0.001102	-6.81077	1.99084
283	5.645	230	503	253009	0.001119	-6.79573	1.98807
288	5.662	230.6	503.6	253613	0.001136	-6.78060	1.98570
293	5.680	231	504	254096	0.001154	-6.76498	1.98413

The linear plot of Kissinger method for tetrapropylammonium tribromide is given in figure 3.

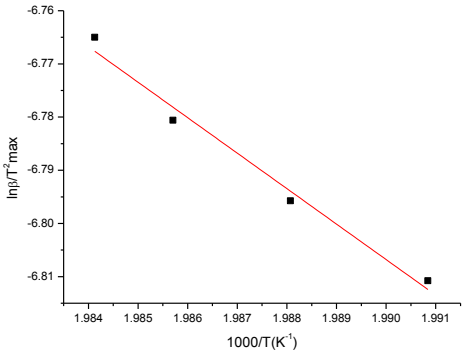

Figure 3. Plot of Kissinger method for **TPATB** at varying degree of Conversions

Thereafter, activation energies for TPATB was also calculated using the Flyn-Wall-Ozawa procedure at varying degree of conversions and the results obtained are given in Table 2.

Table 2. Activation energies for **TPATB** calculated by F-W-O method at varying degree of conversions.

α	TPATB
0.33	2.42
0.70	2.55
0.88	2.75

The iso-conversional plot of *F-W-O* shows a general trend for the activation energy. As an illustration, the iso-conversional plot of *F-W-O* for TPATB is shown in figure 4. From the figure we observed that the fitted lines for the reagent is almost parallel which indicates that the activation energy at different conversions and consequently is almost same, thereby, implying the possibility of a single reaction mechanism (Arora *et. al.*, 2011).

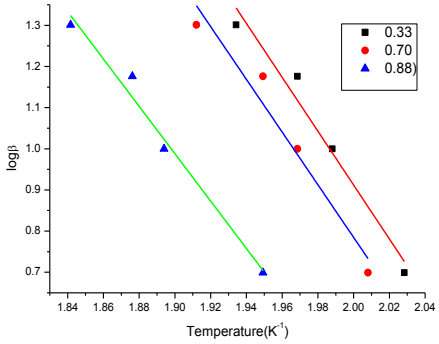

Figure 4. Iso-Conversional plot of F-W-O method for TPATB at varying degree of conversions

The activation energy value calculated by Kissinger method for TPATB is 0.359 kjmol^{-1} with correlation factor r^2 value as 0.97. By comparing the data it can be observed that the order of E_a values calculated by Kissinger method was same as evaluated by initial thermal degradation order i.e. TPATB>TBATB (Kuotsu *et. al.*,2015).

Conclusion

In conclusion it can be said that thermal studies were conducted on tetrapropylammonium tribromide which was synthesized by environmental friendly methods. The purpose of these studies was to understand the basic theory and kinetics of thermal degradation of TPATB. The activation energy values calculated for the reagent also shows that TPATB is more stable than TBATB (Kuotsu *et. al.*,2015).

Acknowledgement: *The author is grateful to UGC for financial support (No. F.5.77/2014-15/MRP/NERO dated 11 March 2015).*

References

Alimenla, B., Kuotsu, B. and Sinha, U. B. (2014). *Chemical Sci. Transactions*. **3(2)**: 826-832.

Anastas, P. T. and Warner, J. C. (2000). Green Chemistry: Theory and Practice, Oxford Univ. press.

Arora, S., Lal, S., Kumar, S., Kumar, M. and Kumar, M. (2011). *Archives of Appl. Sci. Res*. **3(3)**: 188-201.

Askari, F., Barikani, M., Barmar, M., Shokrolahi, F. and Vafayan, M. Iran (2015). *Polym. J.* DOI: 10.10071s13726-015-0367-7.

Badia, J. D., SantonjaBlasco, L., Morina, R. and Greus, R. (2010). *Polym. Degrad. Stab*. **95**: 2192.

Bora, U., Chaudhuri, M. K., Dey, D. and Dhar, S. S. (2001). *Pure Appl. Chem*. **73**: 92-102.

Bose, G., Li, Y., Bhujarbarua, M., Kalita, D. and Khan, A. T. (2001). *Chem. Lett*. **30**: 290.

Burnham, A. K. (2000). *Thermochim. Acta*. **355**: 155.

Chaudhuri, M. K., Bora, U., Dehury, S. K., Dey, D., Dhar, S. S.; Kharmawphlang, W., Choudary, B. M. and Lakshmi Kantan, M. (2004). International Publication Number WO 2004/054962 A1, International Publication Date 01. 07. 2004.

Earnest, C. M. (1984). Anal.Chem. **56**: 1471.

Fraga, F. and Niinez, E. R. (2001). *J. Appl. Polym. Sc.* **80**: 776.

Hamciuc, C., Vlad-Bubulac, T., Petreus, O. and Lisa, G. (2007). *Eur, Polym. J*. **43**: 980.

Jamir, L., Alimenla, B., Kumar, A., Sinha, D. and Sinha, U. B. (2011). *Synth. Commun.* **41**: 147-155.

Kar, G., Saikia, A., Bora, U., Dehury, S. K. and Chaudhuri, M. K. (2003). *Tetrahedron Lett.* **44**: 4503.

Katarzyna, S., Pietro, B. and Francesco, F. (2011). *Third international conference on*

Applied Energy. 1687-1698.
Kavala, V., Naik, S. and Patel, B. K. (2005). *J. Org. Chem*. **70**: 4267-4271.
Kissinger, H. E. (1957). *J. Anal. Chem*. **29**: 1702.
Kumar, A., Alimenla, B., Jamir, L., Sinha, D. and Sinha, U. B. (2011). *Org. Commm*, 1-5.
Kuotsu, N. B., Pongen, C., Phucho, T. and Sinha, U. B. (2015). *Chemical Science Transactions.* DOI: 10.7598/cst 2015.972. **4(1)**: 289-295.
Li, Z., Sun, X., Wang, L., Li, Y. and Ma, Y. (2010). *J. Braz. Chem. Soc*. **21**: 496-501.
Liu, B. Y., Zhao, X. H., Wang, X. H. and Wang, F. S. (2003). *J. of Appl. Polym. Sci.* **90**: 947-953.
Mehran, H., Moshfiqur, R. and Rajender, G. (2015). *International Journal of Chemical Engineering Volume***.** Article ID481739, 1-9.
Meng, X., Huang, Y. D., Yu, H. and Lv, Z. (2007). *Polym. Degrad. Stab*. **92**: 962-967.
Thematic Issue on Green Chemistry, *Chemical Reviews*. (2007). **107**: 2167-2708.
Sun, J. T., Huang, Y. D., Gong, G. F. and Cao, H. L. (2006). *Polym. Degrad. Stab*. **91**: 339-340.
Switala-Zeliazkow, M. (2006). *Polym. Degrad. Stab*. **91**: 1233-1239.
Vyazovkin, S. (2000). *Thermochim. Acta*. 355-155.
Wang, D., Das, A., Leuteritz, A., Boldt, R., Haubler, L., Wagenknecht, U. and Heinrich, G. (2011). *Polym. Degrad. Stab.* **96**: 265.
Wang, D., Das, A., Leuteritz, A., Bolt, R., Haubler, L., Wagenknecht, U. and Heinrich, G. (2011). *Polym. Degrad. Stab*. **96**: 285.

ENVIRONMENTAL IMPACT OF COAL MINING ON WATER BODIES AND NEIGHBOURHOOD OF NAGINIMORA COALMINE, MON, NAGALAND

*Vineetha Pillai, **G. K. Gopesh and ***Meniele K. Nuh
*Department of Chemistry, Kohima Science College (Autonomous), Jotsoma-797002, Nagaland, India
**Bharatiyar University, Coimbatore-641046, India
***Department of Geology, Kohima Science College (Autonomous), Jotsoma-797002, Nagaland, India
e-mail: *Vineethapillai63@gmail.com

Abstract: In the present study the physico chemical characters of surface and ground water of Naginimora coal mine is undertaken. The physicochemical studies like conductivity, turbidity; TDS, COD, total hardness etc. were analyzed. Apart from the above parameters chemical constituents of water like NO_3^-, SO_4^{2-}, Cl^-…… etc were also analyzed, all data are measured in mg/l. Coal mining causes deforestation and soil excavation thereby leads to disturbances in the forest/ ecosystem of the neighborhood. Toxic waste from coal mining zone depletes the aquatic life as well.

Keywords: Permissible limit, toxicity coal mining, parameters, environmental impacts, contamination.

Introduction

Nagaland is blessed with natural resources in which coal plays an important role in the state's economy. The study area bounded by North parallels 26°72' and 27°18' and east meridian 95°30' and 97°07'. It is approximately 60 Km^2 area and falls within the belt of Schuppen and comes within the territorial boundary of Nagaland. The name of this town is derived from the words "Naga Rani Mora" which means "the burial place of the Naga queen". Naginimora coal mine is the first ever coal field in Nagaland, which was founded by the East Indian Company in 1907, almost reaching quasi-centennial anniversary.
In the present study, samples were collected mostly from the running water focusing on the environmental impacts of mining and suitability of drinking water in the surrounding area. The waste materials are being transported in large amount into the streams and nearby rivers. The acidic tailings containment to the ponds, wells, streams etc that may leach into the surrounding farming lands as well. Proper water quality is crucial to the protection of the natural habitats of fish, bugs, birds and plant communities.

Geology of the area

The area of investigation is a plain looking town on the Western bank of Dikhu River. The area is covered by the Barails and Tipams. Coal is exclusively confined to Barail formation along with sandstone and carbonaceous shale. On the basis of their physical properties the coal seems to be of sub- bituminous- Bituminous rank. Besides coal, Barail sandstone occasionally contains iron nodules flattened parallel to bedding. The iron nodules on weathering form concentric layers of limonitic material.

Environmental impact of Coal mining

Mining is necessary for a nation to have adequate and dependable supplies of minerals and materials to meet the power supply, economic and defense needs at acceptable environmental energy and economic costs.

Minerals are nonrenewable resource however the life of mine is finite and mining represents a temporary use of the land. Different techniques are used in mining process, out of which surface mining method is used in the study area. After the coal is removed from the ground , the large amount of waste materials (often very acidic) and particulate emission have lead to major environmental and health hazards to the neighborhood, even to far places through running water streams/rivers. The environmental impact of mining includes erosion, formation of sinkholes, loss of biodiversity and contamination of soil, water by leach out chemicals from mining process.

Water pollution problems caused by mining includes acid mine drainage, metal contamination and increased sediment levels in streams where siltation affects irrigation, domestic water supply, fisheries and other causes. Erosion is also one problem caused by mining. A key cause of landslides around the world is mining. The problem is exacerbated in areas, in which mining activities are uncontrolled and unregulated, a particular issue in the study area. Landslides have great impact, both short-term and long-term, on society and the environment. The short-term impact accounts for loss of life and properties while the long-term impact includes changes in the landscape, including the loss of cultivable land, shifting of population and relocation of populations and establishments causing enormous economic losses and uprooting habitation. The surface topography of the ground over mining excavations plays a key role in the mechanism of subsidence. When a mining operation is performed beneath mountainous or hilly terrain, it may trigger landslides.

All methods of mining affect exist and water quality to a greater extent. Particulate matter is released in surface mining (study area) where overburden is stripped from the site and returned to the pit. When the soil is removed, vegetation is also removed which exposes the soil to the weather causing particulates to become airborne through wind erosion and road traffic. These particulate polluted air can cause respiratory illness like Emphysema, they can even be ingested or absorbed into the skin. However the hazardous nature of pollution is comparatively less in coal mining thn that of clay mining. (Gopash and Vineetha 2017).

Methodology

About 30 samples were collected from surrounding water bodies mostly from streams/ running waters stretching from to 5 to 10Km distance from the Naginimora Mining Zone to access the hydrochemistry and environmental impact of mining. The samples were analyzed for various physicochemical parameters in the laboratory of Centre for Water Resources Development and Management (CWRDM) Calicut, Kerala.

Table1: Important Physicochemical Parameters of running water samples from Naginimora and surroundings (Coal mining area).

Substance or characteristics	Observed values
pH	4.52
Color	Hazen
Turbidity, NTU	50
Total dissolved solids, mg/l	812.06
Total hardness, mg/l	416
Total alkalinity, mg/l	0
Chloride, mg/l	140.81
Sulphate, mg/l	2886.3
Calcium, mg/l	75.08
Magnesium, mg/l	250
Iron, mg/l	150
Sodium, mg/l	31.91
Potassium, mg/l	2.28
Silica (SiO_2), mg/l	5.26
COD, mg/l	268

Results and Discussion

pH: The limit of pH values for drinking water is specified as (6.7- 8.5), the study area water values lies in the range (4.12- 4.54) which shows the acidic character. Abnormal low values of pH in drinking water causes bitter taste to water, which affects mucus membrane, causes corrosion in the carrying pipes and storage vessels and also affects aquatic life.

Turbidity & TDS: Higher values of TDS in ground water are generally not harmful to human beings; however the abnormal higher content of TDS in drinking water may affect persons who are suffering from Heart and Kidney diseases (Geetha et.al 2008). In the present study TDS values lies in the range (704-1472.43).

Total hardness and alkalinity: The samples have relatively higher TDS values with almost zero alkalinity.

Alkalinity is almost reduced to zero maybe due to excess acid drainage to the water bodies. Higher values of hardness maybe due to presence of Ca^{2+}, Mg^{2+},…etc. exceeding the permissible limits causes hardness which leads to the poor lathering with soap and deterioration of clothes. Zero alkalinity values of water samples shows that it is not advisable for drinking and vegetation purpose.

COD: Higher values of COD (50- 300.01) represent the inadequate supply of dissolved oxygen in the samples. However high amount dissolved oxygen imparts good taste to drinking water.

Electrical Conductivity: Electrical Conductivity is a direct function of TDS. Electrical Conductivity values of the samples range from (467-1703µS/cm). Most of the samples show higher conductivity than the prescribed limits by WHO. This higher values maybe due to the high amount of

dissolved inorganic substance in the ionized form.

Si^{2+}: Silicates are in general considered as corrosion inhibitors, because they can deposit protective films on various metal surfaces. A great number of water resources used for water supply occasionally exceed 20mg/L (Tutwill ad Calabrese, 1975) excess sodium in water leads to corrosion of metal pipes. The study area has a low range of Si^{2+} (2.76- 7.38), which may not have any hazardous nature.

Table 2: Comparison of certain physicochemical parameters of samples and standard values of drinking water.

Substance or characteristics	Requirement/ desirable limits	Observed average values from study area
Turbidity,NTU,MAX	10	90
pH	7.5	4.52
Total Hardness (as CaCO3)mg/l	300	812
Calcium (as Ca)2 mg/l, MAX	75	75.08
Magnesium (as Mg) mg/l, MAX	30	250
Iron (as Fe)mg/l, MAX	0.3	150
Manganese (as Mn) mg/l, MAX	0.1	2500
Chlorides (as Cl) mg/l, MAX	250	140
Sulphate(as SO4) mg/l, MAX	150	2886
Nitrate (as NO3) mg/l, MAX	45	149

Fe^{2+}: Fe^{2+} (0.00-200) is one of the main reasons for red color pigmentation to water in the mining zone, which also increases the acidity of water. The excess amount of Iron causes slight toxicity, stringent taste to water and also causes staining of laundry and Porcelain.

Mg^{2+}: Mg^{2+} values (23.59- 72.92) are much higher than the WHO prescribed values. Too high Mg^{2+} adversely affect crop yield as it increases the alkalinity of the soil.

Ca^{2+}: Ca^{2+} values in the study area lie in the range (21.4-279.69). Some samples show bit higher than the limit prescribed by WHO. If it exceeds the limit it can cause incrustation of pipes, poor lathering and deterioration of fabrics.

K^+: K^+ values (0.01-3.99) in water samples are not considered necessary to establish a health based guide line.

Na^+: Sodium salts are generally soluble in water and are leached from terrestrial environment to ground and surface water. In the present study Na^+ values lies in the range (4.03- 98.34). They are non volatile and are thus found in the atmosphere only with particulate matter. Na^+ is ubiquitous in water (WHO bulletine-1996).

NO_3^-, Cl^-, SO_4^{2-}: The study of some water samples in the area show enormous values that range from (24- 150). The higher values of NO_3^- can result in the formation of Nitroso-amines in human body which are carcinogenic in nature.

Cl^- values of the sample (15-154.56) shows bit higher than WHO prescribed values. Higher values of Cl^- enhance acidity of water. SO_4^{2-} value of the samples (68.232-486.35) shows the health hazard caused by water of the area. SO_4^{2-} values shows an alarming environmental concern because of the acidic drainage from the mine area. An amount>400mg/l imparts bitter taste and causes gastro-intestinal irritation.

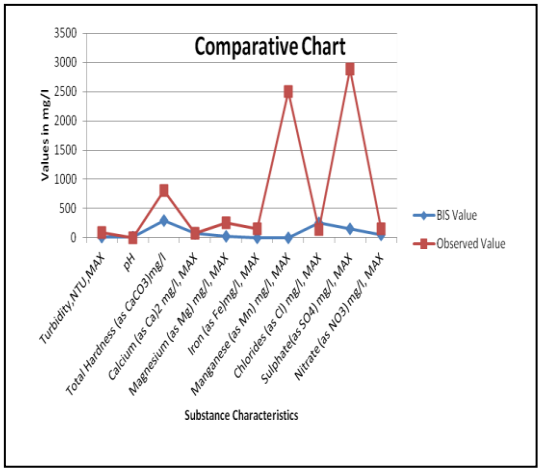

Conclusion

Coal mine generates a number of significant environmental impacts like water quality degradation has posed a great restriction in satisfying local water supply, irrigation to the neighborhood. The acidic tailings containment to the ponds, wells, streams etc that may leach into the surrounding farming lands as well. The present study supports an acidic environment in most of the samples which deteriorate potable and irrigation quality. This Deterioration due to acid drainage is in an alarming state in the study area.

Acknowledgement: *The authors would like to thank The Director, Centre for Water Resources Development and Management (CWRDM), Calicut, Kerala for providing infrastructure facilities for analyzing the samples. The authors also extend sincere gratitude to Professor P. K Rajan, Government College, Kasargodu, Kerala and Hamdok, Senior Block Development Officer, Wokha for their valuable contribution during field survey and sample collection.*

References

Geetha. A, Palani Swamy P. N., Siva Kumar P, Ganesh Kumar & Sujatha (2008). *Journal of Chemistry*. **5(4)**: 696-700.

Gopesh, G. K. & Vineetha, R. (2016). Suitability of drinking of in and around Madai Clay Mining zone, Pazyangadi, Kannur, Kerela.

Tuthill & Calabrese (1975). (EPA, 1996)- Sodium level in spring water, surface and groundwater in Dalmatia, Southern Croatia. 271.

WHO, Geneva (1996). Background document for development of WHO guidelines for drinking water health criteria and supporting information 2nd edition Vol. 2.

STUDY OF THE VARIABILITY OF RAINFALL TRENDS FOR ZUNHEBOTO, DIMAPUR AND MOKOKCHUNG, NAGALAND

*Meripeni Ezung and **Imlisunup Ao
* &** Department of Physics, Kohima Science College (Autonomous), Jotsoma-797002, Nagaland, India.
*e-mail: m_ezung@yahoo.com

Abstract: Variability of rainfall trends for three meteorological observatories at Zunheboto, Dimapur and Mokokchung districts, installed by the Dept. of soil and Water Conservation, Govt. of Nagaland, were studied for a period of 10 years from 2005 to 2014, with the annual rainfall ranging between 623.6 mm to 2675.1 mm. Rainfall distribution over the three stations under study shows maximum rainfall accumulation in Mokokchung and minimum in Dimapur but shows no specific trend in the rainfall pattern during the past decade.

Keywords: Rain Gauge, Rainfall, Zunheboto, Dimapur, Mokokchung.

Introduction

Tropical rainfall comprises more than two thirds of the global rainfall. Excess or deficiency of rainfall causes a lot of suffering which in turn strains the resources. Therefore, study of rainfall, which is the major source of water and its measurements has become one of the important factors in Meteorological studies. For rainfall measurements, many ground based instruments like the Rain Gauge, Disdrometer and Ground-based Rain Radars are used worldwide to study the characteristics of rain. Altogether, there are 15 Meteorological observatories in Nagaland, installed by the Dept. of Soil and Water conservation where Ground based Rain Gauge is used for data collection, spreading all over the state at various altitude ranging from 160 metres (Dimapur) to 1780 metres (Zunheboto) above sea level. In our present study, out of the Rain Gauges installed in 15 observatories, we have chosen three observatories, i.e., Zunheboto, Dimapur and Mokokchung.

The Indian Institute of Science, Bangalore has also analysed the climate change trends in Nagaland at the district level using temperature and rainfall as the key variables for its study. As part of the study, daily rainfall dataset provided by the Indian meteorological department (IMD) was analysed to understand the precipitate trends. The analysis focussed on the monsoon season as more than 95% of the precipitation falls over Nagaland during that period. Majority of the districts of Nagaland experienced an increase in monsoon precipitation for the past 100 years. However one districts showed a decrease in the precipitate of 0.26mm/day and another showed a high increase in the precipitate of 3.96mm/day. In our present study, we will mainly focus on the rainfall patterns for the three observatories and indicate its trends.

Methodology

The Rain Gauge which has been used to collect the data over the three observatories is an instrument used by meteorologists and hydrologists to measure precipitation like rain, snow, hail or sleet in a certain amount of time. It generally measures the precipitations in millimetres which is equivalent to litres per square metre. Rain Gauge amounts are read

either manually or by automatic weather stations (AWS). The frequency of readings will depend on the requirements of the collection agency. The article uses Rain Gauge data to quantify the changes in the rainfall that occurred between 2005 to 2014. The daily rainfall data collected for three Meteorological stations, i.e., Zunheboto, Dimapur and Mokokchung were provided by the Department of Soil and Water Conservation, Government of Nagaland. The annual rainfall and its average for a period of 10 years, from 2005 to 2014 is taken for the analysis and its comparison.

Results and Discussions

It has been observed that over the past 10 years, from 2005 to 2010, the precipitation showed high variability increase in Mokokchung with a maximum rain accumulation amounting to 2675.1 mm while Dimapur showed the minimum. Dimapur also received the minimum rainfall over the past decade with only 623.6 mm. As has been seen by the statistical behaviour, the average annual rainfall amount was higher in the year 2011 and minimum in 2014 but overall only a small variation is seen.

The precipitation trend plots for the three observatories are as shown in figure 1.

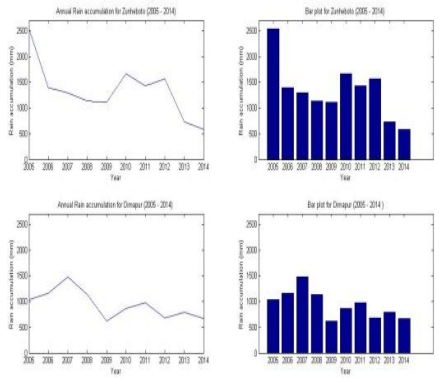

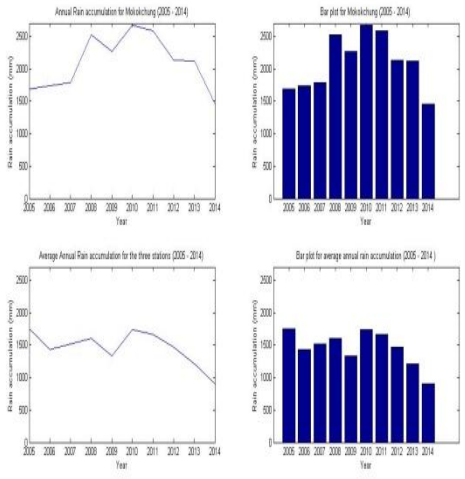

Figure1: Rainfall patterns for Zunheboto, Dimapur and Mokokchung

Basing on the distribution of annual rainfall accumulation collected over the three observatories, the following tabular columns is prepared which shows the distribution of annual and average rainfall:

Table1: Annual rainfall for Zunheboto, Dimapur and Mokokchung

YEAR	R in mm for Zunheboto	R in mm for Dimapur	R in mm for Mokokchung
2005	2530.1	1039.3	1682.9
2006	1393.1	1160.9	1732.3
2007	1293.2	1476.4	1788.4
2008	1133.1	1138.8	2518.3
2009	1108.7	623.6	2267.5
2010	1662.9	863.4	2675.1
2011	1435	981.3	2586.9
2012	1570.6	677.3	2133.5
2013	730.7	796.3	2115.9
2014	579.3	668.1	1455.3

Table 2: Average annual rainfall for Zunheboto, Dimapur and Mokokchung

YEAR	Average R in mm
2005	1750.767
2006	1428.767
2007	1519.333
2008	1596.733
2009	1333.267
2010	1733.8
2011	1667.733
2012	1460.467
2013	1214.3
2014	900.9

Conclusions

From the present study, we observe that the maximum annual rainfall accumulation was in Mokokchung and minimum in Dimapur and the rainfall distribution showed random behaviour in nature. However no specific conclusion can be made as the duration for the present study was only for a short span of 10 years. Seasonal variability also has to be studied thoroughly in detail to understand the nature and its impact on the region and also relate rainfall with agriculture and other sectors.

Acknowledgement: *The authors would like to thank the Department of Soil and Water Conservation, Government of Nagaland for providing meteorological data and to the Principal, Kohima Science College (Autonomous), Jotsoma, for providing necessary facilities to carry out the work.*

References

Geology and Mineral Resources of Manipur, Mizoram, Nagaland and Tripura, Geological Survey of India, 2011.

Krishhnamurthy, V. and Shukla, J. (2000). Intraseasonal and Interannual Variability of rainfall over India. *Journal of Climate***.** 13.

Kurce, B. C. and Singh, Kh. S. (2012). Study of Spatial and temporal distribution of rainfall in Nagaland. *International Journal of Geomatics and Geosciences*. 2(3).

Prof. Ravindranath of the Indian Institute of Science, Bangalore report on the climate profile of Nagaland, sponsored by the German technical aid agency (GIZ) / kreditanstalt für Wiederaufbau (kfW).

Research report submitted by the Government of Nagaland as part of the NSAPCC analysis.

INSTRUMENTS USED FOR MEASURING RAINFALL AND ITS PARAMETERS: AN INTRODUCTION

*Imlisunup Ao and **Meripeni Ezung
* & ** Department of Physics, Kohima Science College (Autonomous), Jotsoma-797002, Nagaland, India.
*e-mail: imlisunupao@gmail.com

Abstract: Study of rain accumulation and its various rainfall parameters which are normally estimated on certain fixed duration of time has gained its interest in meteorological and related fields. Rain parameter measurements are important because the concept of precipitation is still one of the least understood subject in meteorology. In this article, the basic meteorological instruments like the Rain Gauge, Joss Waldvogel Distrometer, Parsivel Distrometer and Micro Rain Radar are discussed briefly along with some limitations. The constraints of non-availability of data for some of the above stated instruments in the same experimental area limits us from comparing and validating the instruments.

Keywords: Rainfall, Rain Gauge, Rain Drop Size Distribution(RDSD), Joss Waldvogel Distrometer (JWD), Parsivel Disdrometer, Micro Rain Radar (MRR).

Introduction

Historical background

The earliest record of rainfall data were kept by the Ancient Greeks, about 500 B.C ago. The Indians in about 400 B.C also used the rainfall records to correlate against the expected growth. In 1441, during the reign of King Sejong the Great of the Joseon Dynasty of Korea invented the Cheugugi, which was the first standardized Rain Gauge. The tipping bucket Rain Gauge was first created by Christopher Wren in 1662 in Britain in collaboration with Robert Hooke. But it was Richard Towneley who first made the systematic measurements of Rainfall over a period of 15 years from 1677 to 1694. For rainfall measurements, many ground based instruments like the Disdrometer, Rain gauge and Ground-based Rain Radars are used worldwide to study the characteristics of rain. Using the Disdrometer, many researchers have studied the rain drop size distributions (RDSD) and its characteristic parameters like, Drop size distribution N(D), Liquid water content (LWC) and Rain rate (RR). With the importance of rainfall measurements, RDSD has become an important parameter to be studied.

Accurate rain rate estimation requires detailed knowledge of RDSD. All the rain parameters have integral dependence on the RDSD and study of RDSD has been found to be applicable in areas like the microwave communication, satellite meteorology, soil erosion and cloud physics.

We will discuss some of the instruments which are in use to study Rainfall and its parameters.

Rain Gauge

Precipitations in the form of rain, snow, hail or sleet over a given amount of time are measured using Rain Gauge. It generally measures the precipitations in millimetres which is equivalent to litres per

square metre. The observations of a Rain Gauge is read either manually or by automatic weather stations (AWS). The precipitation is not retained in most cases, however some stations use the rainfall and snowfall records for obtaining the level of pollutants over that area. Rain Gauges should be placed in an open area where there are no obstacles, such as buildings or trees to block the rain. This is to prevent the water collected on the roofs of buildings or the leaves of trees from dripping into the Rain Gauge after the rain, resulting in inaccurate readings. Some important limitations of a Rain Gauge are:

a. Attempting to collect rain data in a hurricane can give unreliable data due to wind extremes.
b. The indication of Rainfall from Rain Gauges is only for a localized area.
c. Underestimated rainfall records are possible due to the drops sticking to the sides of the collecting device.
d. Blocking of subsequent rain due to collection of ice or snow in the Gauge when the outside temperature is at or below freezing point.

Usually a tapering funnel of copper or polyester of standard dimension allows the rain water to collect in an enclosed bottle or cylinder for subsequent measurements. The Gauge is set up in an open ground with the funnel rim up to 30 cm above the ground surface. Some Gauges are calibrated in such a manner that the amount of rainfall is read directly while the others are calculated from the depth of water in the container along with the dimensions of the funnel.

The second type of rain gauge is the autographic gauge which can be either of the tilting-siphon type or the tipping-bucket type as shown in Fig (1). The recording chart on an autographic rain gauge is mounted on a drum which is driven by clockwork and typically rotates round a vertical axis once per day as shown in Fig (2). For a tilting-siphon rain gauge, the rainwater in a collector displaces a float so that a marking pen attached to the float makes a continuous trace on the paper. The two buckets in a tipping-bucket rain gauge rest on a pivot so that when one bucket has received 0.2 (or 0.5 mm) of rain, it dips by gravity, empties the rainwater and allows the other bucket to start its collection. During the tip, an electrical switch is closed and triggers a nearby autographic recorder to register each 'tilt', thus giving a fairly continuous record of precipitation.

Fig 1: Exterior of a tipping bucket Rain Gauge

Fig 2: Tipping bucket Rain Gauge recorder chart

Distrometer

Disdrometers are instruments used for measuring Rain drop size distribution and its parameters. The early Distrometers were the ground-based flour type and the filter paper method type. Subsequently, different techniques were developed like, the impact-type Distrometer, radar-type Distrometer, laser-optical-type Distrometer, the advanced 2D video Disdrometer, etc. We will focus mainly on the Joss- Waldvogel Distrometer (JWD), which is an impact type of Distrometer and Parsivel Distrometer, which is a laser-optic type. Study of the RDSD provide important information for the microphysical behaviour of precipitation and its statistical distribution.

Description and principle of operation of the JWD Disdrometer

Developed by Joss and Waldvogel in 1967, the JWD is an impact type of instrument, consisting of a sensor head and signal processing electronics, used for determining the size, in terms of the equivalent diameter of the raindrops and the integral rain parameters continuously. The JWD is one of the most used instruments for analyzing the RDSD. The surface cross sectional area of the instrument is 50 cm^2 . It measures drop diameter ranging from 0.3 to 5.3 mm. The instrument transforms the impacting vertical raindrop samples into an electric pulse whose amplitude is a function of the drop diameter. The arrangement contains the processor and the sensor as shown in Fig 3. A cable of length 20 metre long is used to connect the sensor and the processor.

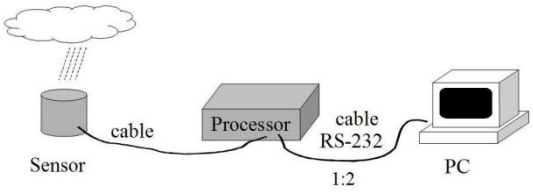

Fig 3: Schematic arrangement of the processor and the sensor in a Distrometer setup.

The main functions of the processor are to supply power to the sensor and processes the signal from the sensor. It also contains circuits for testing the performance of the instrument. It is connected to a PC, which receives the datas through a program. The sensor which is exposed to the raindrops to be measured produces an electric pulse for every drop hitting it. In the processor, these pulses are divided into different classes of drop diameter, which are combined into certain drop size classes for obtaining statistically meaningful samples and for every drop hitting the sensor, a seven bit ASC11 code is transmitted to the serial interface of the PC. The output data from the Disdrometer is connected directly to the PC and the data cable from the Disdrometer is logged every minute to the PC. An in-build programme in the Distrometer enables the users of the Disdrometer to record and evaluate the drop size measurements with the PC.

Some limitations of JWD are:

a. Underestimation of small drops in the presence of background noise and electrical interference.
b. The Distrometer cannot distinguish large drops of the order >5mm in diameter.
c. During heavy rain, small drops are underestimated. This is called the Distrometer's dead time.
d. Number of drops with diameter less than D_{min} (>0) are not recorded by the Distrometer.

Description and principle of Parsival Distrometer

The Parsivel Distrometer is a laser based optical Distrometer for simultaneous measurement of **PAR**ticle **Si**ze and **VEL**ocity of all liquids and solid precipitation. Parsivel operates in any weather regime and the incorporated heating device minimizes the negative effect of freezing and frozen precipitate. The instrument provides a full picture of the precipitation event in all weather phenomena and provides accurate reporting of precipitation types and intensities without degradation of performance in severe outdoor environments. It is also a low cost, durable and reliable instrument, thus making it suitable for small-scale variability study in RDSDs. The size of the measurable liquid precipitation particles ranges from 0.2 to 8 mm and for solid precipitation particles, ranges from 0.2 to 25 mm. The precipitation particles can be in the form of drizzle, drizzle with rain, rain, Rain or drizzle with snow, Snow, Snow grains, Soft hail or hail. The Parsivel Distrometer consists of a special sensor head which measures and detects the precipitation optically and a fast digital signal processor which processes and stores the data as shown in Fig 4. A laser sensor produces the horizontal strip of light and the precipitating particles passing through the laser beam will block off a portion of the bean corresponding to their diameter, reducing the output voltage. This process will determine the size of the particles. When the particle enters the laser beam, a signal starts and this signal ends when the particle leaves the laser beam. The duration of this signal determines the speed of the particles. Parameters like spectrum size, precipitation type, kinetic energy, precipitation intensity, Radar reflectivity and visibility are derived from the determined size and speed of the precipitation particles. The instrument supports meteorological observations and weather services for improving severe weather forecasts and warnings for thunderstorms, snow and ice conditions, flood forecast and warnings, supports to aviation and road traffic. The radar reflectivity coefficient along with ground based precipitation data improves the regional weather forecasts and high water early warning system.

Fig.4: Parsivel Distrometer setup

Limitations of Parsivel Distrometer are:

a. The parsivel Distrometer tends to underestimate drop size < 2.00 mm.
b. The observations from the lower bin size cannot be measured accurately due to low signal-to-noise ratio.
c. The vertical profiles of rain parameters cannot be determined by this ground based instrument.
d. The Parsivel Distrometer may record erroneous measurements due to wind turbulence and splashing.

Rain radar

Radar is used by meteorologists to study the rain and its characteristics. It has

become an important tool for short term weather forecasting and research on severe weather phenomenon. The term RADAR is an acronym for Radio Detection And Ranging. It is a system for detecting the position, movement, and nature of remote objects by means of radio waves reflected from its surface. The principle of radar involves the transmission of pulses of electromagnetic waves by means of a directional antenna. The pulses that are intercepted by the objects are reflected and recorded by a receiver. It is then processed electronically and converted into the requisite format by means of a display device. In Doppler radar, the velocity of the object is measured by applying the Doppler principle.

Rain radar is limited to a certain frequency band of electromagnetic waves. A large wavelength creates errors due to radar beam interaction with ground and from vertical variation of the reflectivity. Moreover, the problem linked to attenuation become critical for short wavelength. Thus, a proper choice of the wavelength becomes very crucial for weather radars. S-band radar units are commonly used in the USA because the primary use of the radar information is to assess large areas (Crum et al., 1993). In the European combined coverage systems both C and S band are used: for example the German Weather Service DWD privileged a C –band radar network (Bartels and Weigl, 1998) the French National Network use C and S band radars, and selected S-band radars for the south region concerned with heavy storm events. Different rain radars are used for research related works according to the needs and nature of the studies. Indeed, high resolution data for rainfall estimation is the need of the hour for further breakthrough in atmospheric physics. Vertically pointing Doppler radars (VPRs) are mainly used to investigate the vertical profile of rainfall and Drop Size Distributions (Peters et al.2005). We will limit our discussion for the vertically pointing Doppler radar known as Micro Rain Radar (MRR).

Micro Rain Radar

The Micro Rain Radar (MRR) is a compact FM-CW Doppler radar for measuring the vertical profiles of drop size distributions in the height range of around 15m to 6000m. The RADAR antenna is an offset parabolic dish with vertical beam orientation allowing rainwater to drain without building pond as shown in Fig 5. The high resolution in time and height enables the MRR to monitor the genesis of frozen hydrometeors, the melting zone (bright band) and the formation of raindrops. The MRR has been adapted even for monitoring of avalanches and volcanoes. The advantage of Micro Rain radar is to detect rain parameters below the threshold of conventional equipments due to its high sensitivity and fine temporal resolution. The main component of the MRR is a frequency modulated gunn- diode-oscillator with integrated mixing diode and nominal transmit power of 50 mw.

Fig 5: Micro Rain Radar

The radiation is transmitted vertically into the atmosphere where a small portion is scattered back to the antenna from rain drops or other forms of precipitation. There is a frequency deviation between the transmitted and the received signal due to the falling velocity of the rain drops. This Doppler frequency is a measure for the falling velocity of the rain drops. Thus, the backscattered signal consists of a distribution of different Doppler frequencies due to different diameters of the drops falling with different falling velocities. The resultant spectrum yields a power spectrum which is spread over a range of frequency lines corresponding tothe Doppler frequencies of the signal. The reflectivity spectrum is calculated from the mean power spectrum processed by the Radar Control and Processing Device (RCPD). A linearly decreasing saw tooth modulation of the transmit signal processes the profile measurements with selectable range resolution.

The number of drops per volume and diameter which is termed as drop size distribution can be expressed as

$$N(\mathrm{D},\mathrm{i}) = \frac{\eta(D,i)}{\sigma(D)} \qquad (1)$$

Where $\eta(D,i)$ the spectral reflectivity density with respect to a rain is drop of diameter (D) and $\sigma(\mathrm{D})$ is the corresponding backscattered cross section. The value of $\eta(D,i)$ can be obtained from the Doppler velocity as

$$\eta(D,i) = \eta(\mathrm{v},i)\frac{\partial v}{\partial D} \qquad (2)$$

Where the relation between terminal fall velocity (v) in ms^{-1} and drop diameter (D) in mm is obtained by using a generalized form of Gunn and Kintzer relation (1949)

$$v\,(\mathrm{D}) = [9.65 - 10.3\{\exp\ [-0.6\mathrm{D}]\}]\,\delta v(h) \qquad (3)$$

Where a height dependent density correction for the fall velocity ($\delta v(h)$) for second order approximation is estimated by using the Foote and du Toit (1969) relation. By appropriately weighted integration of the spectral reflectivity density, various integral rain parameters are obtained as illustrated herewith.

Radar reflectivity factor Z($mm^6\ m^{-3}$) is represented by Rayleigh approximation as

$$Z = \int_0^\infty N(D)\,\mathrm{D}^6 dD$$

The equivalent radar equivalent factor (Z_e) for MRR is,

$$Z_e = \frac{\lambda^4}{\pi^5 |K|^2}\int_0^\infty \eta(f)\,df$$

Where K = m^2 +1 and m is the complex refractive index of the water droplet at the radar frequency while λ is the radar wavelength.

The liquid water content (LWC) is proportional to the 3rd moment of the DSD as

$$LWC = \rho_W \frac{\pi}{6}\int_0^\infty N(D)D^3 dD$$

Similarly, the rainfall rate R(mm/h) is expressed in terms of the DSD as

$$R = \frac{\pi}{6}\int_0^\infty N(D)D^3 v(D)dD$$

Where v(D) is the raindrop fall velocity. The other rainfall parameters are also calculated in the same way.

The MRR furnishes output files like the 'Raw data' which is the primary data available in a time interval of every 10 second. The second type of data is the processed data which is obtained every 10 second after processing the raw data. This estimates the DSD and other rainfall parameters. The third file is the average data which is similar to the processed data file, but is averaged over 60 second.

Limitations of MRR are discussed below:

a. The MRR experiences severe attenuation during heavy rain.
b. The MRR does a volume measurement compared to devices observing point measurements. This may create some discrepancy for comparative studies.
c. The accuracy of MRR is influenced by strong vertical wind and turbulence.
d. The MR data are limited to small temporal and spatial variations.
e. The MRR data are sometimes unrealistically high or have missing value due to failed estimation of noise and attenuation.
f. The algorithm developed for calculation of DSD is applied normally for the size range of 0.246 mm to 5.03 mm corresponding to the height-normalized velocity range of 0.75 m/s $\leq$ v / δv(h) $\leq$ 9.25 m/s. This normally gives an underestimation of rain droplet less than 0.246 mm and greater than 5.03 mm.

Conclusions

Meteorological records are a valuable resource for knowledge and the study of Rainfall measurements and its parameters is of great interest not only from Ancient times but it is a subject which has gained its importance even in recent times. Its applications can be found in various fields like Hydrology, Meteorology, Remote sensing, Radio Communication and most importantly in Agriculture. The problem of soil erosion, rain washing of the atmosphere, coalescence and collision breakup, interaction between raindrop and atmospheric components, interaction between rainfall and electromagnetic waves etc depends on the microstructure of rain. The microstructure of the rain which is in turn dependent on the RDSD and rainfall parameters can be studied by making use of the various meteorological instruments. However, the discussion on all the instruments is beyond the scope of this article. Further studies with the requisite data need to be performed in order to prove its applicability and limitations in practice.

Acknowledgement*: The authors would like to the Principal, Kohima Science College (Autonomous), Jotsoma for providing the necessary facilities to carry out the work.*

References

Atlas, D., Srivastava, R. and Sekhon, R. (1973). Doppler radar characteristics of precipitation at vertical incidence. *Rev. Geophys. Space Phys*. **11**: 1-35.

Gunn, R. and Kintzer, G. (1949). The terminal velocity of fall for water droplets in stagnant air. *J. Meteor*. **6**: 243-248.

Marzuki, H. Hashiguchi, T. shimomai, I. Rahayu, M., Vonnisa and Afdal. (2016). Performance Evaluation of Micro Rain Radar over Sumatra through comparison with Disdrometer and wind profiler. *Progress in electromagnetic research M.* **50**: 33-46.

Marzuki, M., Hashiguchi, H., Yamamoto, M. K., Mori, S. and Yamanaka, M. K. (2013). Regional variability of raindrop

size distribution over Indonesia. Ann. Geophysics. **31**: 1941-1948.

Peters, G., B. Fischer, H. Munster, M. Clemens, A. and Wagner. (2005). Profiles of raindrop size distribution as retrieved by micro rain radars. *J. Appl. Meteor*. **44**: 1930-1949.

Raupach, T. H. and Berne, A. (2015). Correction of rain drop size distribution measured by Parsivel Didtrometer, using a two-dimensional video Disdrometer as a reference. Atmos. Meas. Tech. **8**. 343-365.

Tokay, A. and Bashor, P. G. (2010). An experimental study of small-scale variability of raindrop size distribution. *J. Appl. Meteorology and Climatology*. **49**: 2348-2365.

You, Cheol-Hwan, Lee, and Dong-In. (2015). Decadal variation in raindrop size distributions in Busan, Korea. *Advances in Meteor*. 1-8.

SHAPE ANALYSIS OF PALAEOGENE DISANG- BARAIL TRANSITIONAL SEQUENCE IN PARTS OF KOHIMA SYNCLINORIUM, KOHIMA DISTRICT, NAGALAND, NORTH-EAST INDIA

*Lily Sema and **Ralimongla
* & **Department of Geology, Kohima Science College (Autonomous), Jotsoma-797002, Nagaland, India
e-mail: *dr.lilyazha@gmail.com , **dr.ralimongla@gmail.com

Abstract: The study of shape analysis reflects the degree and intensity of the process of selective sorting and maturity of the sediment. There are two concepts regarding the shape of the sedimentary particles, these are sphericity and roundness. The changes in the hydrodynamic condition of transport are shown by changes in shape. Roundness and sphericity analysis of about 1500 detrital quartz grains has been carried out for the Palaeogene Disang-Barail Transitional Sequence of the Kohima Synclinorium. The detritus of the quartz grains shows subrounded to subangular grains with low values of sphericity indicating maturity of the sediments and distant as well as close proximity of provenance to the depositional site.

Keywords: Shape, Roundness, Sphericity, Palaeogene, Disang-Barail Transitional Sediments (DBTS), Kohima Synclinorium

Introduction

The study area (fig.1) is bounded by Latitudes 25^0 32' N – 25^0 36' N, and Longitudes 94^0 05'E – $94^0$10'E of the topographic sheet no. 83 K/2 of survey of India. It forms a part of the Kohima Synclinorium and is 4 kms south of Kohima (Lat. 25^0 40' N; Long. 94^0 08'E), the capital town of Nagaland state bordering Manipur in the NE India.

The sediments in the study area do not exhibits lithological characteristics of the Disang Shales or the Barail sandstones. The eastern half of the area is dominated by shales which pass gradationally into succession having higher increment of sandstone beds as seen along the contact between the Disang Shales and the Barail sandstones elsewhere (Fig.2). However multistoreyed sandstone units having similar attributes as those of the Barails are found to be overlain by thick succession of shales resembling Disangs at places. Due to the mixed lithological character of the sediment, the lithological units of the area have been considered to be part of the Disang-Barail Transitional Sequence (DBTS) (Pandey and Srivastva, 2000 and Srivastva, 2001).

Geological Setting

Morphotectonically, Nagaland is divisible into three units; the Schuppen Belt in the west, the Inner Fold Belt in the middle and the Naga Metamorphics along with the Ophiolite and associated sediments in the east (Mathur & Evans, 1964). The most prominent structural unit in the Inner Fold Belt is the Kohima Synclinorium, a part of which forms the present area of investigation, its western limits are defined by Halflong-Disang thrust and the eastern limits by Changrung-Zungki-Lainye thrust respectively (Naik, 1998). The northern limb of this synclinorium forming the Barail ranges of North Cachar, extends south-westward below Halflong and westward, fringing the eastern

extension of Meghalaya plateau. The southern limb extends into west Manipur, East Cachar and East Mizoram. The core of the synclinorium is occupied by the Surma basin (Chakrabarti and Banerjee, 1988). Lithological similarity in the two limbs does not exist according to Nandy D.R. (1974). Sandstones are dominant in the Barail rocks of the Barail range whereas the predominant units in the southern limb are the shales. The outer most ring of Kohima Synclinorium south of Halflong is the underlying Disangs displaying a sequence of splintery shales with minor sandstones (Rao, A.R, 1983).

Methodology

Mineralogical maturity of sediments is known from the sphericity and roundness of sedimentary particles. The most abundant and physio-chemically resistant clastic detrital mineral in sandstone is quartz. It is therefore used as index mineral to study the shape and roundness of sedimentary particles. Krumbein (1941) stated that the abrasion and wear that is directed on the sediments intensely alters its roundness; meanwhile shape contributes to the selective transport and settling velocities of the particles. The processes of abrasion, solution and sorting action on the sediments alter the shape and roundness of the grains (Pettijohn, Potter & Seiver, 1972). According to Wadell (1932), roundness and sphericity are two geometrically distinct concepts. Roundness exhibits the abrasional history of the clastic particles whereas sphericity indicates the depositional condition during moment of accumulation (Pettijohn, 1984). These properties are seen in the larger grains but rarely in fine sand and silt (Friedman and Sanders, 1978). Wentworth (1919) introduced first the quantitative system of measuring the shape of the sand grains. The shape of a particle contributes immensely in the selective transport and hydrodynamic behavior of the transporting agent towards the settling velocity of a particle affected by its shape (Boggs, 1967). Depending upon the changes in the hydrodynamic condition of the transport the changes in the size, shape and sphericity of the sediments develops. The shape of the sediment is controlled by the original shape, structure and endurance of the fragments, the nature and impact of the physical and chemical action it is subjected and the duration and distance through which the action extends. For the study of the maturity of the sediments, sphericity and roundness of the clastic quartz grains are used. Discrimination of depositional environment (Patro and Sahu, 1971, 1977) and multi group linear discrimination between depositional environments (Sahu, 1982 b) are developed by using sphericity and roundness of detrital quartz grains.

Roundness analysis

According to Power M.C (1953) roundness is independent of shape but is dependent on the sharpness of the edges and corners of the fragments. Wentworth (1919), for the first time, defined roundness as

$$r_i / R$$

Where, r_i = ratio of the radius of curvature of the sharpest edges and

R = one half of the longest diameter.

Roundness analysis of about 1500 detrital quartz grains from the six lithofacies identified in the study area has been carried out, following the method suggested by Power (1953). Clastic quartz was classified into different roundness classes and average

roundness of each sample was calculated by the method suggested by Anger (1963).

If n_1, n_2, n_3, n_4, n_5, n_6 are number frequencies corresponding to six roundness classes, then

$$\text{Average roundness} = \frac{n_1m_1 + n_2 m_2 + n_3 m_3 + n_4 m_4 + n_5 m_5 + n_6 m_6}{Sn}$$

Where, Sn = $n_1+n_2+n_3+n_4+n_5+n_6$ and $m_1+m_2+m_3+m_4+m_5+m_6$ denote mid points of each roundness class interval.

Table.1 shows the average roundness for different facies of Palaeogene sediments of the study area. Most of the detrital quartz grains are found to be subangular to subrounded. The grains also exhibits bimodal character of the sediments with respect to roundness when frequency and roundness values are used to draw the cumulative curve (Table 2a, Fig.3) and histograms (Table2a, Fig. 4).

Roundness values (Table.3) of Palaeogene sediments vary from 0.30 to 0.44 averaging 0.37 (subrounded). The plot against the average roundness values and average sphericity (Fig. 5) are found to be closely packed showing close trend between the two. The average values of mean, median and standard deviation of roundness are 0.34, 0.34 and 0.04 respectively while for sphericity it is 0.29, 0.28 and 0.05 respectively.

The study of the roundness values of the Palaeogene sediments reveals that the quartz grains are subrounded to subangular. The subrounded detrital grains are indicative of prolonged transportation or a distant source and the subangular grains from older sediments of nearby area. According to Friedman and Sanders (1978), selective sorting separates rounder grains from less rounder ones. Well rounded grains may also be result of many cycles of transport or intensive abrasion in a special environment with formation of angular grains from marginal source (Pettijohn, Potter and Seiver, 1972). Krumbein and Sloss (1963) stated that roundness of grain is a measure of sedimentary maturity. Therefore dominance of subrounded grains in the present case indicates that the sediments are matured in nature.

Sphericity analysis

Wadell (1932) developed the concept of sphericity and defined sphericity as the ratio between the diameter of the sphere with same volume as the particle and the diameter of the circumscribed sphere. Krumbein and Pettijohn (1938) measured sphericity by using the formula,

Sphericity = dc /Dc

Where, dc = the normal diameter of the grain projection
Dc = the diameter of the smallest circumscribing circle

Sneed and Folk (1958) proposed maximum projection sphericity which is the ratio of the cross sectional area of a sphere of the same volume as the particle divided by its maximum projected area. This is quantitatively defined as

$$\psi_p = \sqrt{S^2} / LI$$

Where, S = the short axis
L = the long axis
I = the intermediate axis of the grain

The clastic quartz grains of the Palaeogene sediments show sphericity values from 0.24 to 0.37. The lower sphericity values suggest a shorter transportation of the sediments.

The C/B values of the quartz grains are also low ranging from 0.21 to 0.33 averaging 0.27. According to Spalletti (1976) C/B values tend to increase with transportation distance. Since the C/B values of the sediments are low it is suggestive of shorter transportation. Cumulative curves (Table. 2b, Fig.6) and the histograms (Table. 2b, Fig.7) of frequency against sphericity values exhibit bimodality of the sediments in respect of sphericity. This suggests transportation of the Palaeogene sediments under fluvial regime (Russel and Taylor, 1937).

Conclusion

The overall shape analysis of the detritus for the Palaeogene Disang-Barail transitional sequences shows subrounded to subangular grains with low values of sphericity. This indicates that the sediments are matured and have come from distant source as well as from older sediments of nearby area.

Table: 1 Average Sphericity and Roundness values of clastic quartz grains of the Palaeogene Disang-Barail transitional sediments.

Sample number	Sphericity	Roundness	C/B
L2	0.35	0.37	0.32
L3	0.27	0.34	0.25
L4	0.30	0.38	0.29
L7	0.28	0.27	0.24
L9	0.24	0.35	0.22
L11	0.27	0.34	0.26
L12	0.30	0.38	0.28
L13	0.25	0.36	0.24
L15	0.28	0.39	0.27
L17	0.32	0.39	0.30
L18	0.27	0.38	0.23
L19	0.25	0.35	0.21
L21	0.27	0.39	0.26
L22	0.30	0.36	0.29
L23	0.25	0.33	0.22
L25	0.27	0.37	0.23
L26	0.28	0.36	0.27
L27	0.37	0.40	0.31
L28	0.25	0.30	0.21
L31	0.35	0.39	0.30
L32	0.25	0.37	0.22
L33	0.37	0.42	0.32
L34	0.27	0.44	0.26
L36	0.35	0.42	0.33
Average	**0.29**	**0.37**	**0.27**

Table: 2a Size range, frequency% and cumulative % of Roundness in the Palaeogene Disang-Barail transitional sediments.

Range	Grains	Frequency	Cumulative %
0.28-0.30	202	8.416	8.416
0.30-0.32	226	9.416	17.832
0.32-0.34	410	17.083	34.915
0.34-0.36	744	31.000	65.915
0.36-0.38	315	13.125	79.040
0.38-0.40	104	6.833	85.873
0.40-0.42	179	7.458	93.331
0.42-0.44	160	6.666	99.997

Table: 2b Size range, frequency% and cumulative % of Sphericity in the Palaeogene Disang-Barail transitional sediments.

Range	Grains	Frequency	Cumulative %
0.24-0.26	436	18.166	18.166
0.26-0.28	568	23.666	41.832
0.28-0.30	307	12.791	54.623
0.30-0.32	257	10.708	65.331
0.32-0.34	266	11.083	76.414
0.34-0.36	347	14.458	90.872
0.36-0.38	219	9.125	99.99

Table: 3 Roundness frequency distribution(%) of the detrital quartz grains in six lithofacies of the Palaeogene Disang-Barail transitional sediments.

Sl.no	0.12-0.17	0.17-0.25	0.25-0.35	0.35-0.49	0.49-0.70	0.70-1.00
Lithofacies 'A'						
L10				0.42		
L29				0.40		
L31				0.39		
L33				0.42		
L34				0.44		
Lithofacies 'B'						
L24				0.36		
L26				0.36		
L27				0.40		
L28			0.30			
Lithofacies 'C'						
L9			0.35			
L12				0.38		
L13				0.36		
L17				0.39		
L19			0.35			
L36				0.42		
Lithofacies 'D'						
L2				0.37		
L6				0.38		
L7				0.37		
L8				0.38		
L18				0.38		
L25				0.37		
L32				0.37		
Lithofacies 'E'						
L1			0.34			
L3			0.34			
L11			0.34			
L15				0.39		
L16				0.39		
L20				0.39		
L21				0.39		
Lithofacies 'F'						
L4				0.38		
L14				0.35		
L22				0.36		
L23			0.33			
L35			0.35			

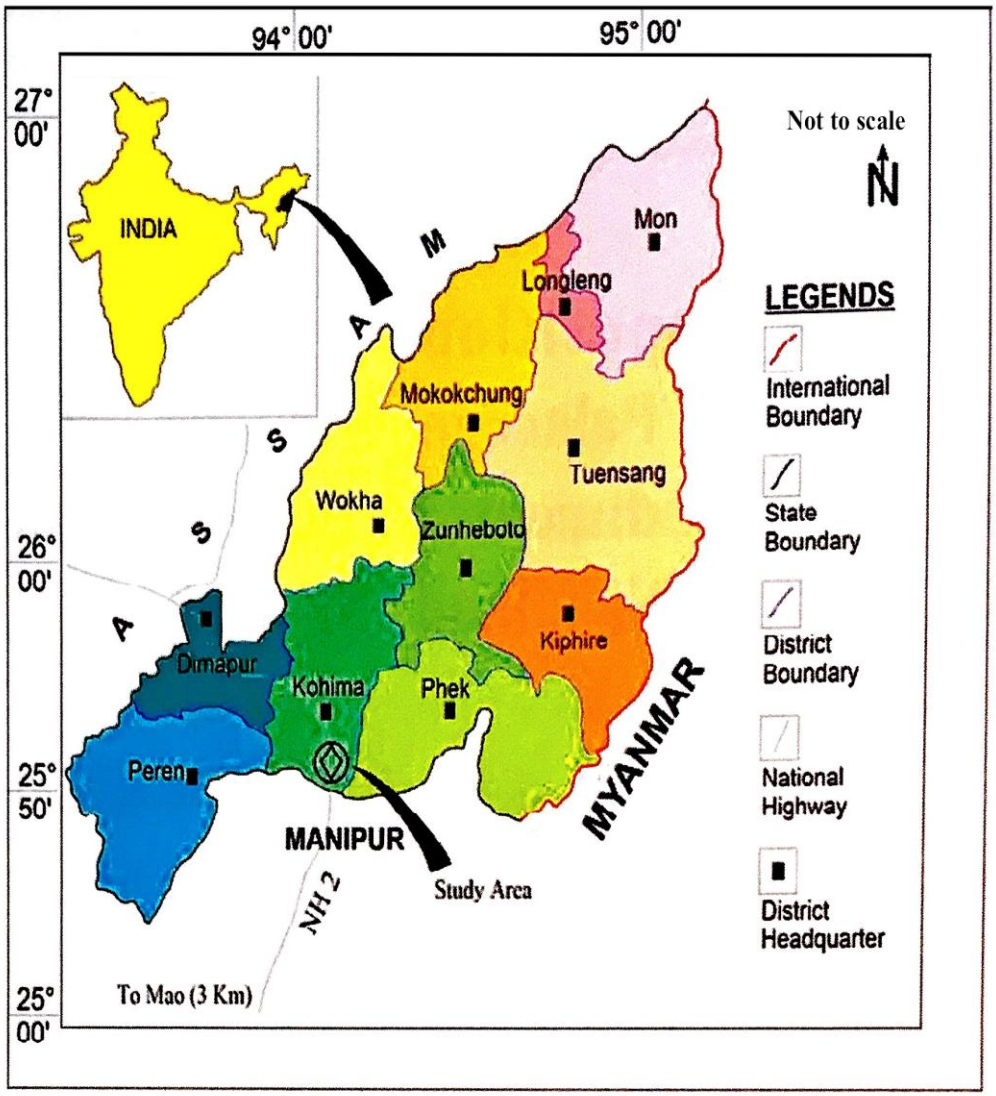

Fig. 1: Location of the study area.

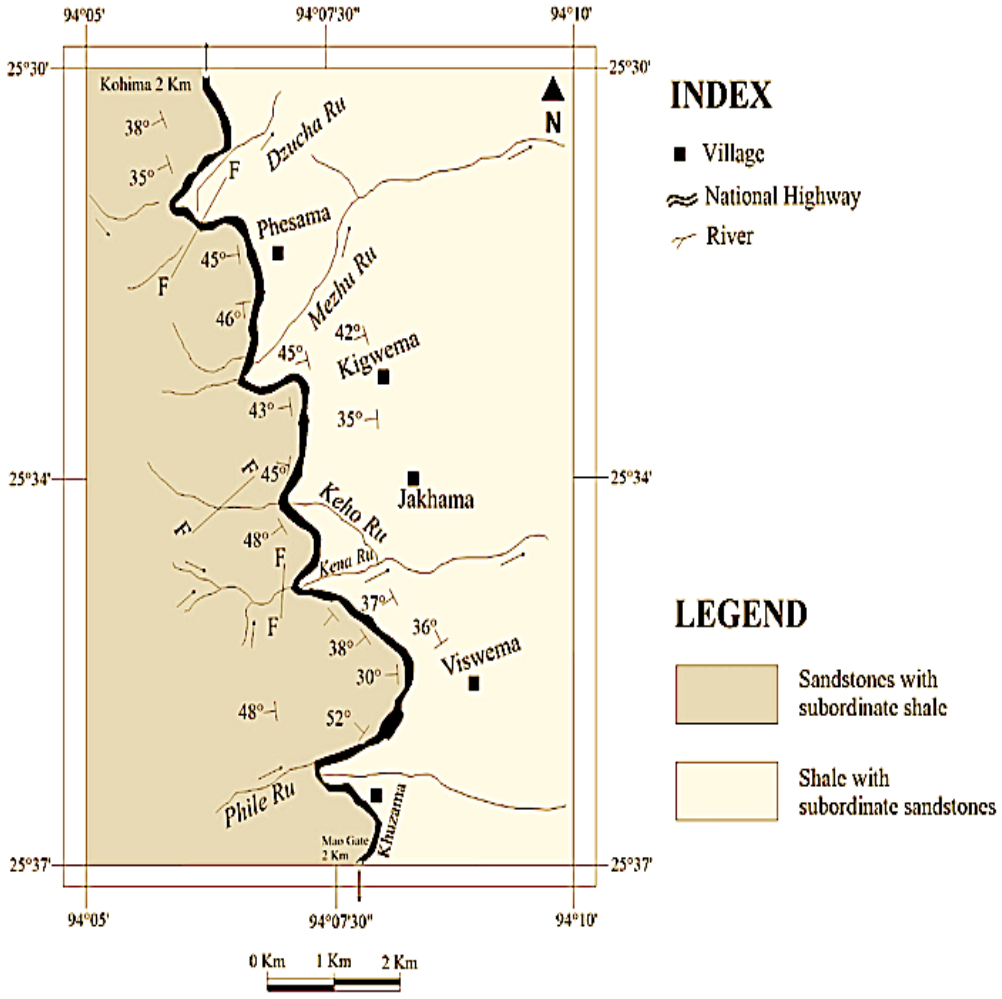

Fig : 2 Geological map of the area

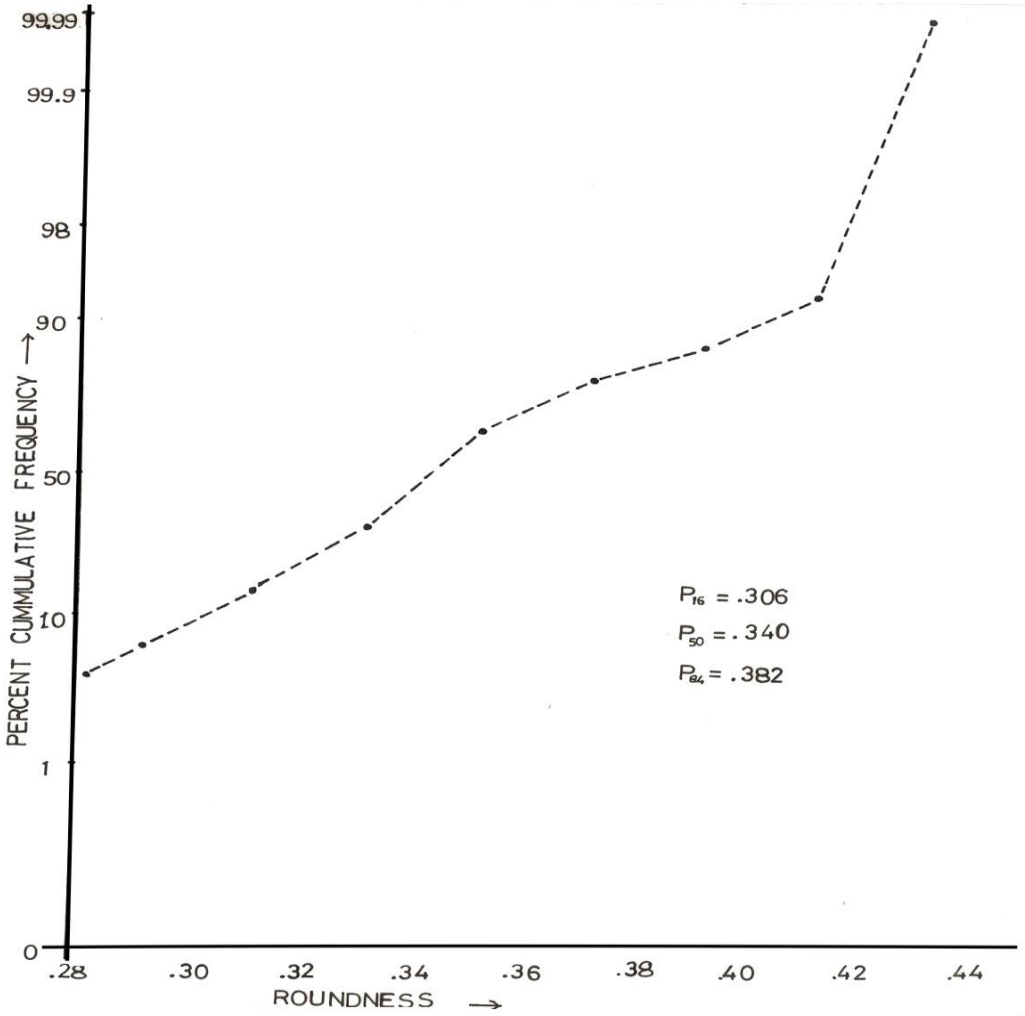

FIG: 3 Percentage cummulative distribution of roundness in the Palaeogene Disang - Barail Transitional Sediments.

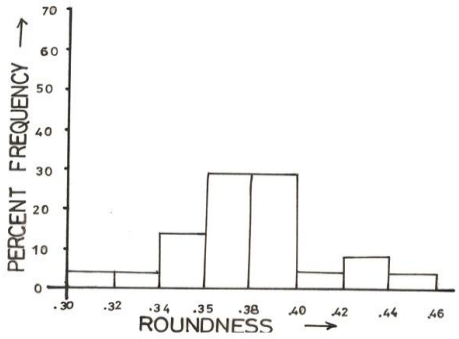

FIG:4 FREQUENCY DISTRIBUTION OF ROUNDNESS IN THE PALAEOGENE DISANG-BARAIL TRANSITIONAL SEDIMENTS.

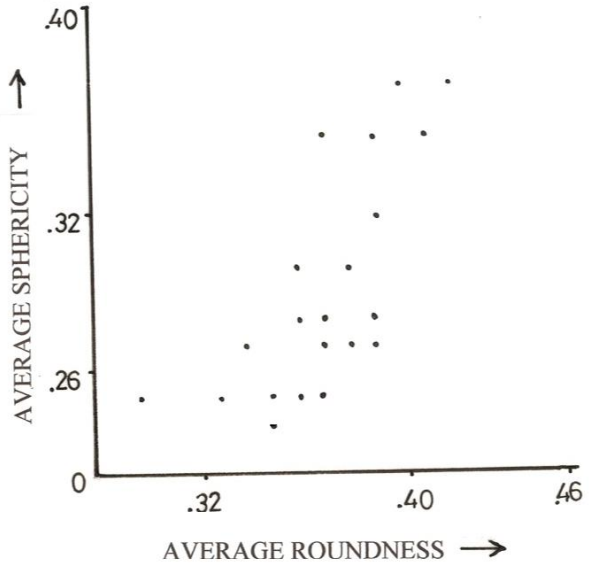

FIG:5 Average roundness versus average sphericity for the Palaeogene Disang-Barail Transitional Sediments.

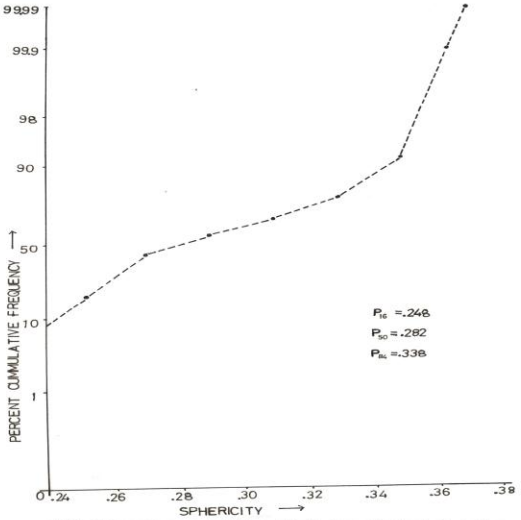

FIG: 6 Percentage cumulative distribution of sphericity in the Palaeogene Disang- Barail Transitional sediments.

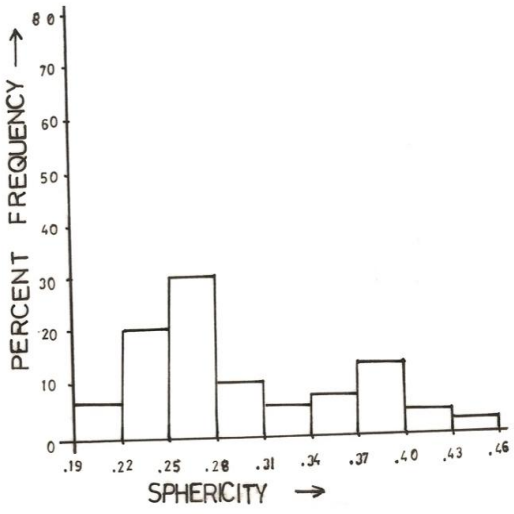

FIG:7 Frequency distribution of sphericity in the Palaeogene Disang- Barail Transitional Sediments.

References

Boggs, Sam, Jr. (1967). Measurement of roundness and sphericity parameters using an electronic particle size analyzer. *Jour. Sed. Pet.* **37**: 908 -913.

Friedman, G. M. and Sanders, J. E. (1978). Principles of Sedimentology, New York, Wiley and Sons Inc, Canada. 792.

Krumbein, W. C. and Pettijohn, F. J. (1938). Manual of sedimentary petrography. New York. Appleton Century Co. 549.

Krumbein, W. C. (1941). Measurement and geological significance of shape and roundness of sedimentary particles: *Jour. Sed. Pet.* **11**: 64-72.

Krumbein, W. C and Sloss. (1963). Stratigraphy and Sedimentation. 600. W.H. Freeman San Francisco.

Naik, G. C. (1998). Tectonostratigraphic evolution and palaeogeographic reconstruction of Northeast India. *Proc. Indo-German Workshop on Border Strandlogy magnetostratigraphy pilot project, Calcutta.*

Nandy, D. R. (1974). Geological mapping and mineral survey in parts of Mizoram. *Unpublished G.S.I. Prog. Report (FS 1971 - 72).*

Patro, B. C. and Sahu, B. K. (1971). Frequency distribution of sphericity and roundness data of quartz grain on weight basis. *Ind. Mineralogist.* **12**: 33-39.

Patro, B. C. and Sahu, B. K. (1977). Discriminant analysis of sphericity and roundness data of clastic quartz grains in river, beach and dune. *Sed. Geol.* **19**: 301-311.

Pettijohn, F. J., Potter, P. E. and Siever, R. (1972). Sand and sandstones. Heidelberg, Springer-Verlag. 61.

Pettijohn, F. J., Potter, P. E., and Siever, R. (1987). Sand and sandstones. Heidelberg, Springer-Verlag.

Power, M. C. (1953). A new roundness scale for sedimentary particles. *Jour. Sed.Pet.* **23**: 117-119.

Pettijohn, F. J. (1984). Sedimentary rocks, 3rd edition. CBS Publishers, New Delhi.

Rao, A. R. (1983). Geology and hydrocarbon potential of a part of Assam-Arakan Basin and adjacent regions. *Petroleum Asia Journal.* **6(4)**: 127-158.

Russell, R. D. and Taylor, R. E. (1937). Roundness and shape of Mississippi river sand. *Jour. Geol.* **45**: 235-267.

Sahu, B. K. (1982b). Multigroup discrimination of river, beach and dune sands using roundness statistics. *Jour. Sed. Pet.* **52**: 779-784.

Sneed, E. D. and Folk, R.E. (1958). Pebbles in the Lower Colorado River, Texas. A study of particle morphogenesis. *Journal of Geology.* **66**: 114-150.

Spalletti, I. A. (1976). The axial ratio, C/B as an indicator of shape selective transportation. *Jour. Sed. Pet.* **46**: 243-248.

Wadell, H. (1932). Volume, shape and roundness of rock particles. *Jour. Geol. V.O.* 443-451.

Wentworth, C. K. (1919) A laboratory and field study of cobble abrasion. *Jour. Geol.* **277**: 507-521.

Address for correspondence:
Principal
Kohima Science College (Autonomous),
Jotsoma- 797002
Nagaland

Rüsie: A Journal of Contemporary Scientific, Academic and Social Issues
Vol. 4, 2017
ISSN 2348-0637

The journal (Rüsie) is published annually.

The views and opinions expressed by the authors are their own statement. They do not reflect the opinion of the college authority and editorial board. The college will assume no responsibility for the statement of the contributors.

RÜSIE

Translation: 'A movement for a cause' is the literal translation of the Tenyidie word **'Rüsie'**. It is a movement of united action and efforts by a group or a community for a specific purpose.

The name 'Rüsie' befits the journal which is also a movement for a cause- of Science and Social issues. A forum to disseminate ideas and knowledge through united and collective efforts.

Name of the journal proposed by Dr Shürhozelie Liezietsu, President, Ura Academy.

FORMAT GUIDELINES

1. Length of the article- maximum 8 pages (A4 size paper), with a font size of 11 and a line spacing of 1.0 (single) in two columns (max. 1500 words).
2. Font style: Times New Roman (preferably typed in Microsoft Word)
3. Headings:
   i) Title
   ii) Abstract (max. 50 words)
   iii) Introduction
   iv) Objectives
   v) Methodology
   vi) Results (preferably with figures and tables in science section)
   vii) Conclusion
   viii) Acknowledgement
   ix) References
   x) Brief bio-data of the author(s)
4. Articles to be submitted in soft copy to the Chief Editor (mhathungy@gmail.com)